Non-invasive Single Cell Metabolic Trajectories Using the Phasor-FLIM method

Michelle A. Digman, Ph.D.
Associate Professor,
mdigman@uci.edu
Department of Biomedical Engineering
Joint Associate Professor, Department of Chemical & Biomolecular Engineering
Joint Associate Professor, Department of Developmental and Cell Biology

Co-I, P41, Laboratory for Fluorescence Dynamics (LFD)
Director, W.M. Keck Nanoimaging Lab

Overview of the Lab

Metabolic Alterations

Embryo Development
Neurodegeneration
Cancer

Mechanobiology and the Influence of ECM on Metabolism in Cancer Cells

Mitochondrial recruitment
Tumor organoids

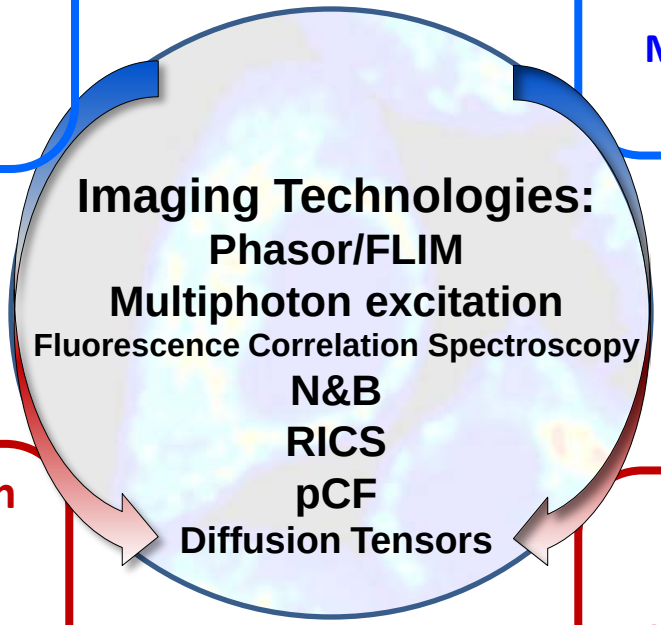

DNA Damage and Protein Phase Transitions in Health and Disease

Protein dynamics and distinct physical states

Signal transduction dynamics during epidermal wound healing and partial Epithelial-to-Mesenchymal Transition

Non-invasive tissue fluorescence imaging technique:

- Cellular fluorescence imaging enables researchers to see the effects of cellular, structural, and/or metabolic activity by observing the in response to light excitation

- Natural tissue fluorescence is caused by intrinsic “fluorophores”.

Important Tissue Fluorophores:

- Collagen
- Elastin
- Keratin
- NADH
- FAD
- Porphyrin
- Fibrin

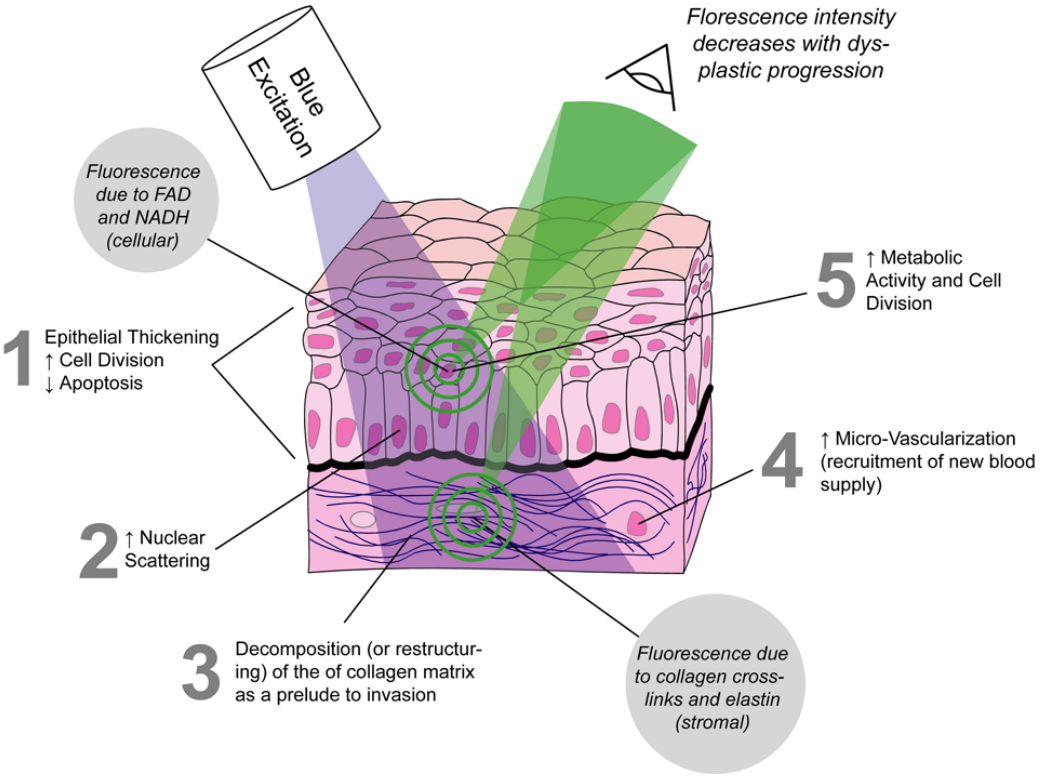

http://biophotonics.bccrc.ca/index.php/research/technologies/afi/

2-photon excitation offers the capability to infiltrate deeper in living tissues

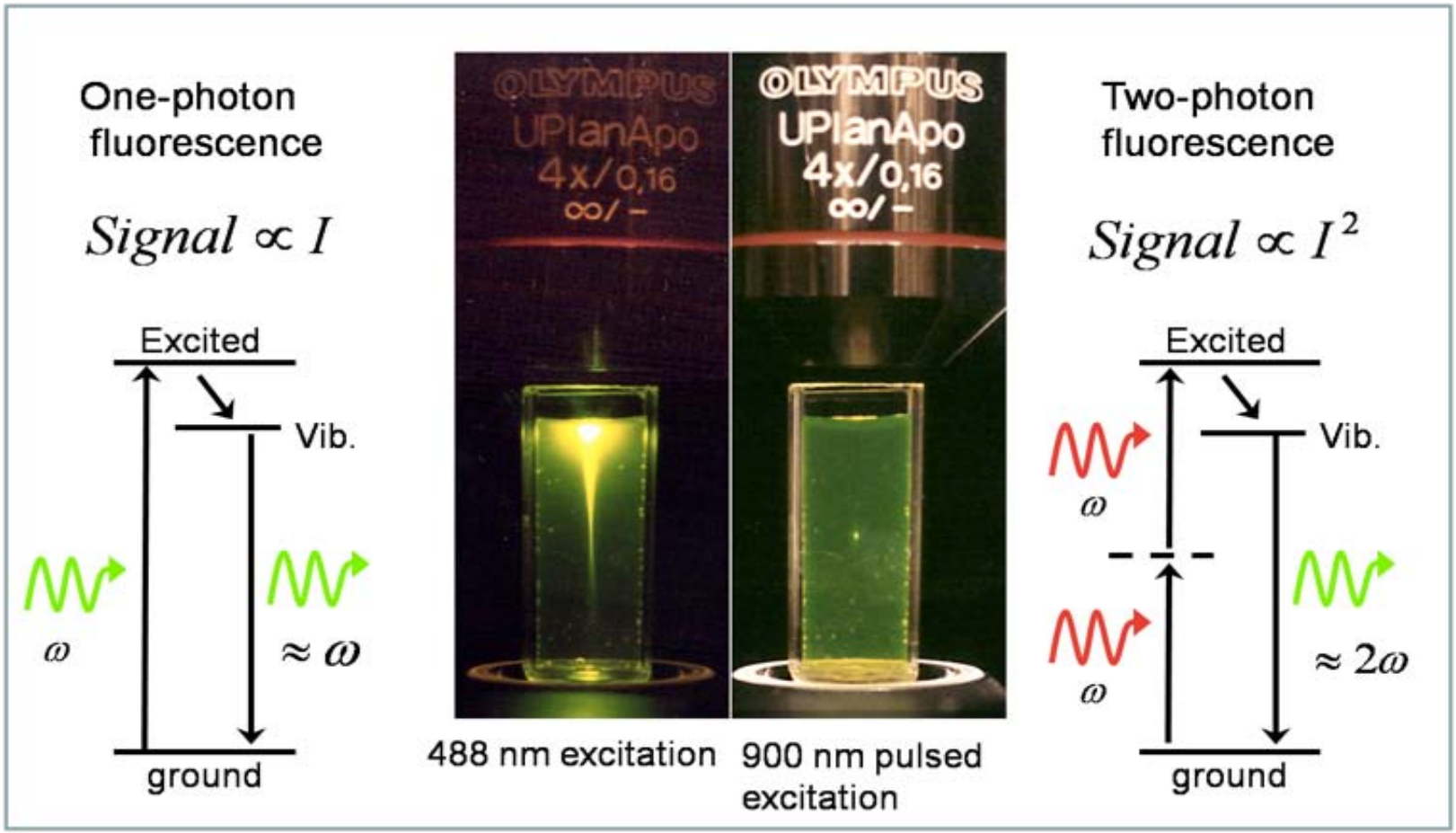

How: Two Photons of half the energy (twice the wavelength), if temporally coincident, sum their energies (2x05=1x) to drive fluorophore to activated state (NOTE: This requires very high powered, very expensive lasers)

Fluorescence lifetime imaging microscopy (FLIM)

- While conventional fluorescence microscopy separates fluorophores by wavelengths, FLIM separates sources by fluorescence lifetime.
- The fluorescence lifetime is the average time that a molecule spends in the excited state before emitting a photon.

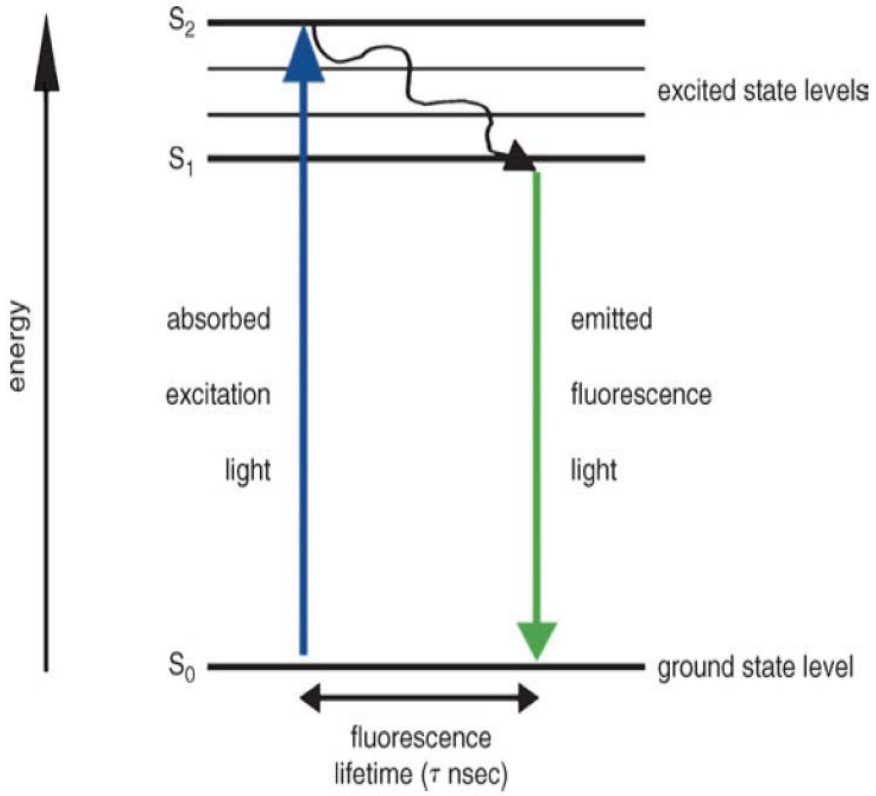

Lleres, D., Swift, S., & Lamond, A. I. (2007). Detecting protein-protein interactions in vivo with FRET using multiphoton fluorescence lifetime imaging microscopy (FLIM). *Current protocols in cytometry*, 12-10.

Outline

- What is Fluorescence Lifetime imaging Microscopy (FLIM)?
- How is fluorescence lifetime measured in the time domain versus the frequency domain?
- How is a FLIM system set up?
- What are the advantages/disadvantages of FLIM?
- The phasor analysis for FLIM
- Metabolic trajectories of living systems

Why we do FLIM?

FLIM is used for :

- FRET (Forster Resonance Energy Transfer).
- Intracellular mapping of Ion concentration and pH imaging.
- Biochemical reactions (oxidation/reduction) processes
  - NAD and NADH. Metabolic index.
- Long lifetime imaging (phosphorescence).
  - For example O_2 concentration in the cell or in tissues

Time Resolved Fluorescence

- What's happening during the time of the fluorescence emission?

- Fluorescence Lifetime

Fluorescence Quantum Yield φ: important for dyes
Ratio of the rate of fluorescence and the sum of the rates that depopulate the excited state

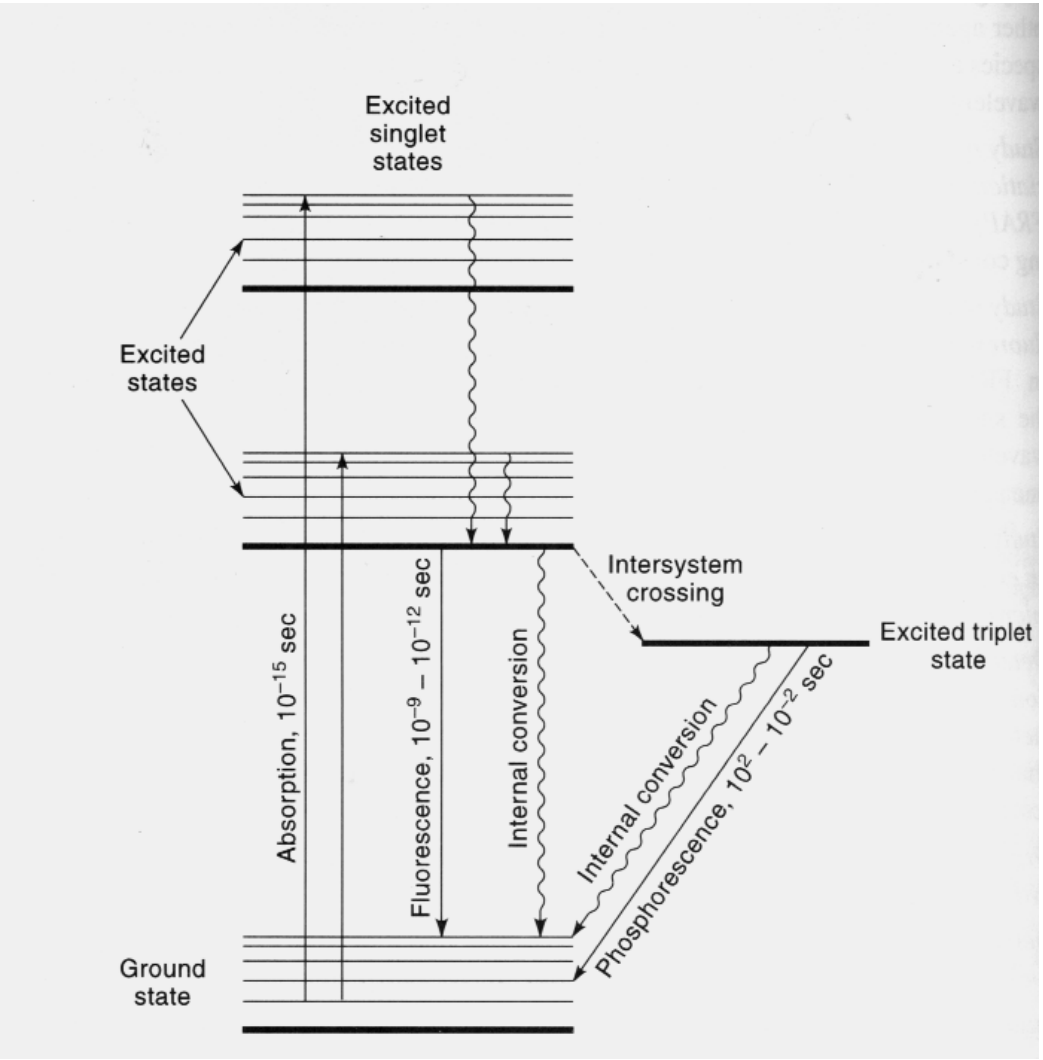

Quantum Yield:

Can be expressed as the lifetime

$$\phi = \frac{k_f}{k_f + k_{isc} + k_{nonrad}}$$

$$\tau_0^{-1} = k_f$$

Natural lifetime:
Inverse of the fluorescence emission rate

$$\tau^{-1} = k_f + k_{isc}$$

Measured lifetime is sum of
Rates of natural lifetime
and non radiative decay paths

Fluorescence Lifetime τ

Although we often speak of the properties of fluorophores as if they are studied in isolation, such is not usually the case.

Absorption and emission processes are almost always studied on *populations* of molecules and the average properties of a molecule of the population are deduced from the macroscopic properties of the process.

The rate of the change of molecules in the excited state depends on how much you depopulate the emission plus how much you populate because of excitation

Illustration:

A laser beam passes through a solution containing fluorophores. At any given time some fluorophores will be excited, while the rest will be in its ground state.

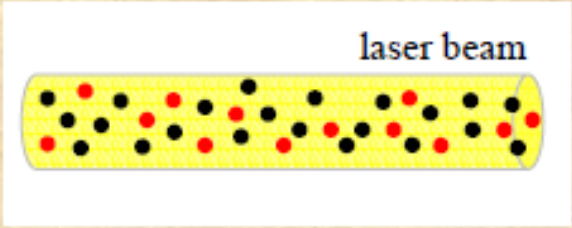

The excited state population of fluorophores is described by a rate equation:

$$\frac{dn^*}{dt} = -n^* \Gamma + n\, f(t)$$

where $n + n^* = n_o$ (n_o describes the total number of molecules and is a constant)

Meaning of the lifetimes

- Imagine that a sample is excited with an infinitely sharp pulse of light
- This results in an initial population (n_0) of fluorophores in the excited state
- The excited-state population decays with a rate of $\Gamma+k_{nr}$:

$$\frac{dn(t)}{dt} = (\Gamma + k_{nr})\, n(t)$$

n(*t*) is the number of excited molecules at time *t* following excitation, Γ is the emissive rate and k_{nr} is the nonradiative rate.

Because emission is a random event, and each excited fluorophore has the same probability of emitting in a given period of time, the result is an exponential decay of the excited state population :

$$n(t) = n_0 \exp(-t/\tau)$$

Measuring fluorescence lifetime using a field programmable gate array (FPGA)

- Our approach uses serial detectors in the photon counting mode, and the digital heterodyning method to acquire data which is directly analyzed in the frequency domain.
- the sampling windows slide through the entire period of the emission response due to the slight difference in frequencies, for a total of 256 steps

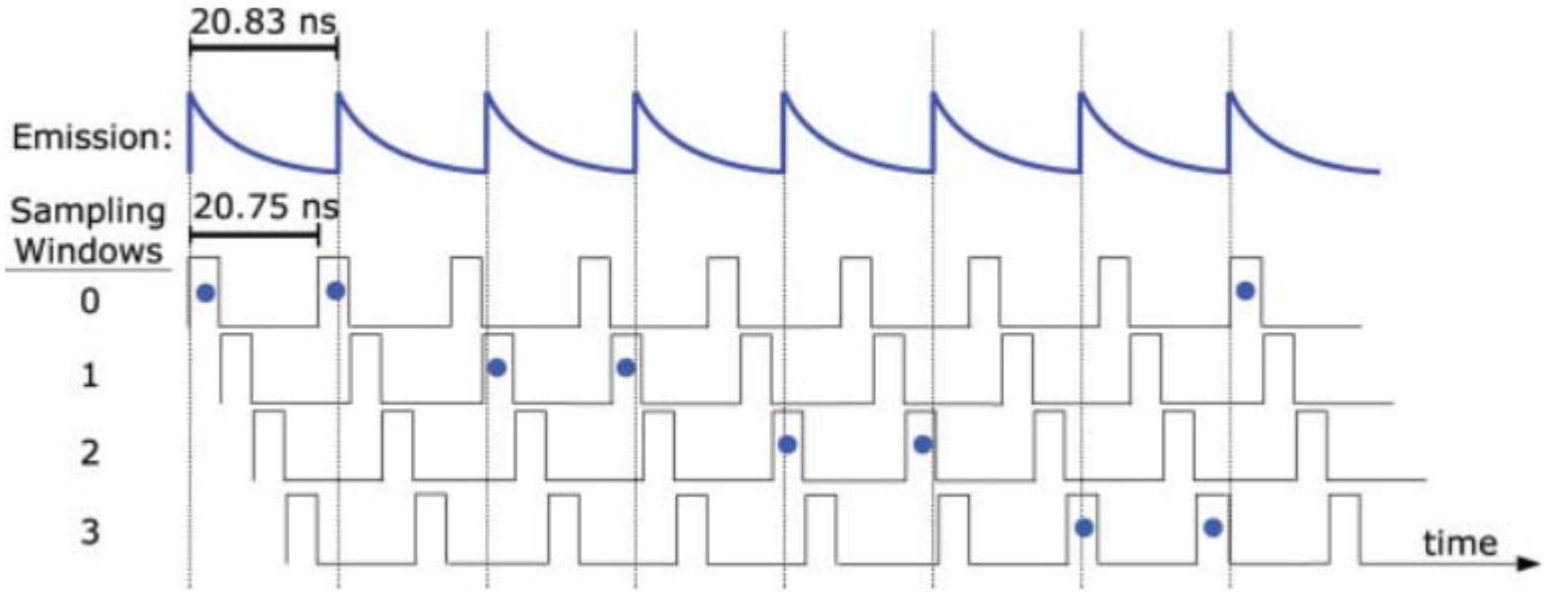

illustration of the digital heterodyning principle
Colyer et al.

Colyer RA, Lee CY, Gratton E. Microsc Res Tech. 2008; 71(3): 201-213.

Phasor - A Graphic Representation of the Raw FLIM Data

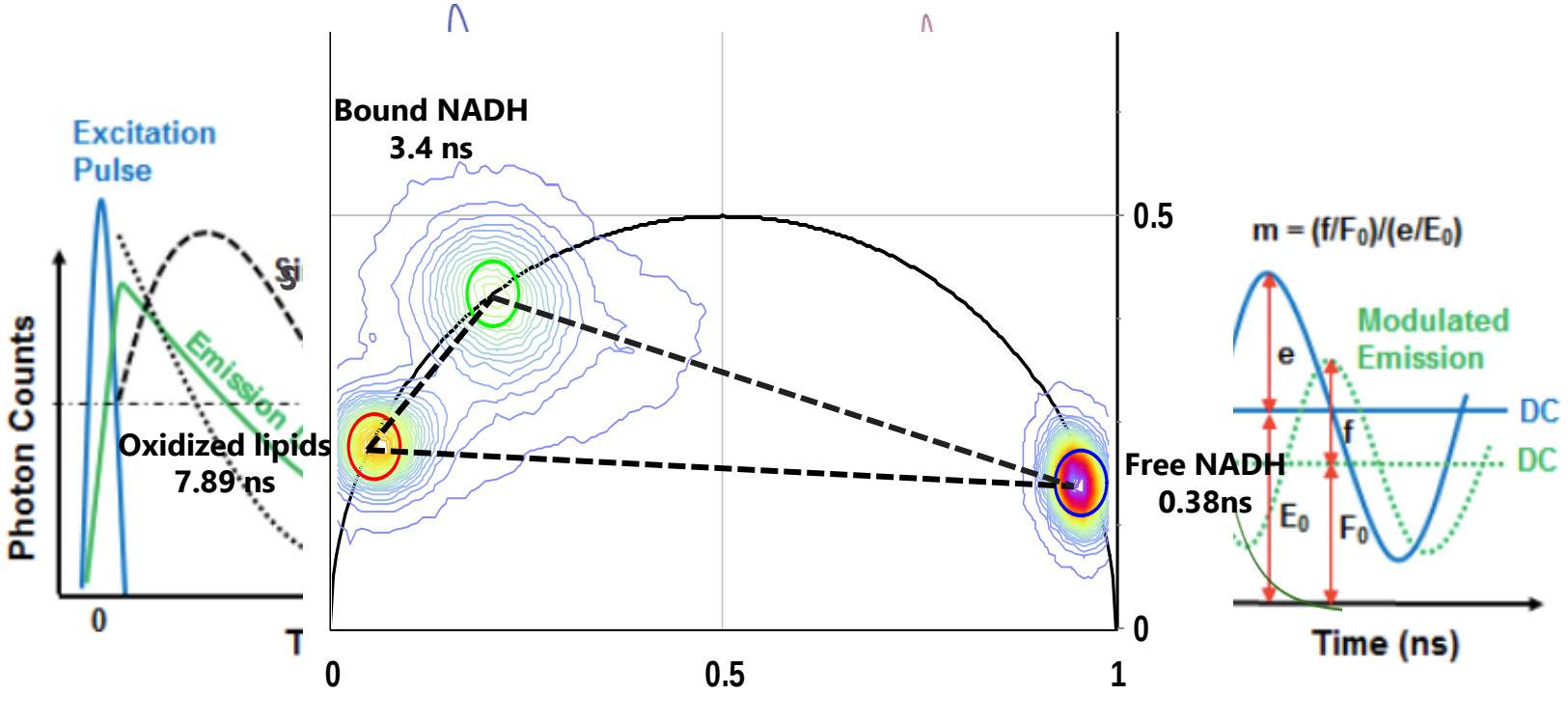

$$g_i(\omega) = \int_0^\infty I(t)\cos(\omega t)dt \,/\, \int_0^\infty I(t)dt$$

$$s_i(\omega) = \int_0^\infty I(t)\sin(\omega t)dt \,/\, \int_0^\infty I(t)dt$$

$$g(\omega) = m\cos(\varphi) \quad s(\omega) = m\sin(\varphi)$$

Digman M.A. et al Biophys J. 2008; 94(2): L14-16. PMC2157251

Using Phasors: what is a phasor??

$$g_i(\omega) = \int_0^\infty I(t)\cos(\omega t)dt \,/\, \int_0^\infty I(t)dt$$

$$s_i(\omega) = \int_0^\infty I(t)\sin(\omega t)dt \,/\, \int_0^\infty I(t)dt$$

- A phasor is a quantity like a vector. Phasors is the addition of amplitudes using vectors. They can be added. You need to calculate the vector components and then add the components to obtain the vector sum

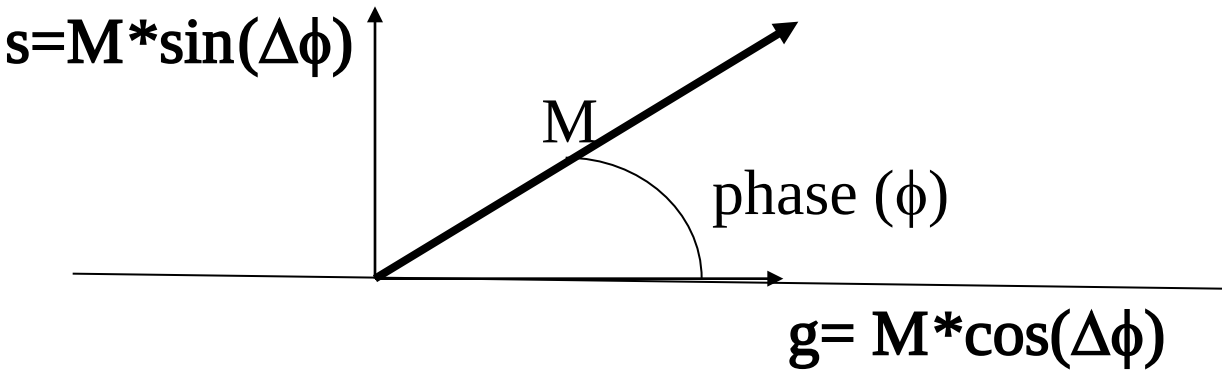

NOTE: s and g are obtained automatically from the Fast Fourier Transform (FFT) of the time domain

The addition of amplitudes using vectors

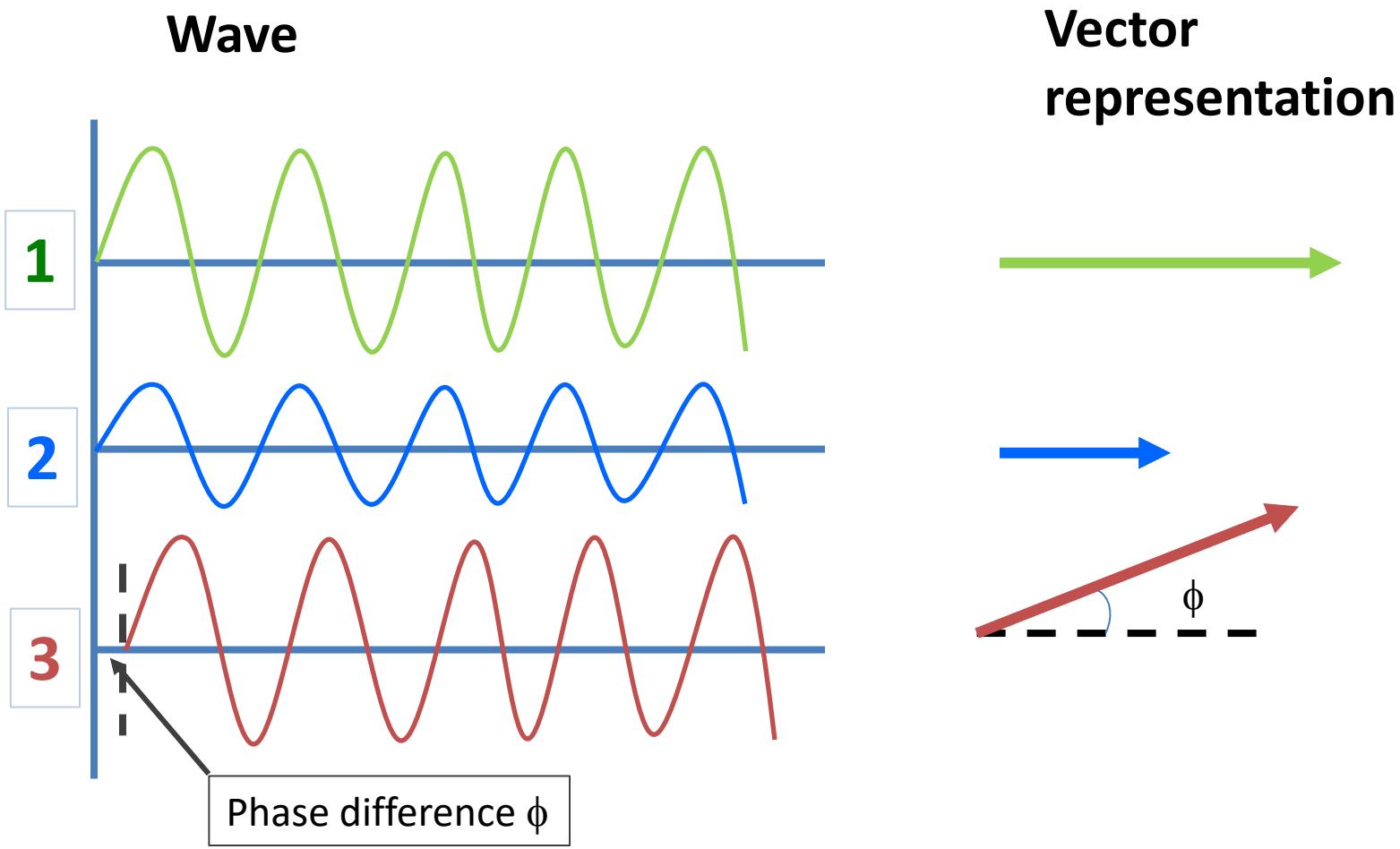

Amplitude of the wave ~ Magnitude or length of the vector
Phase of the wave ~ Direction of the vector

The addition of amplitudes using vectors

Wave

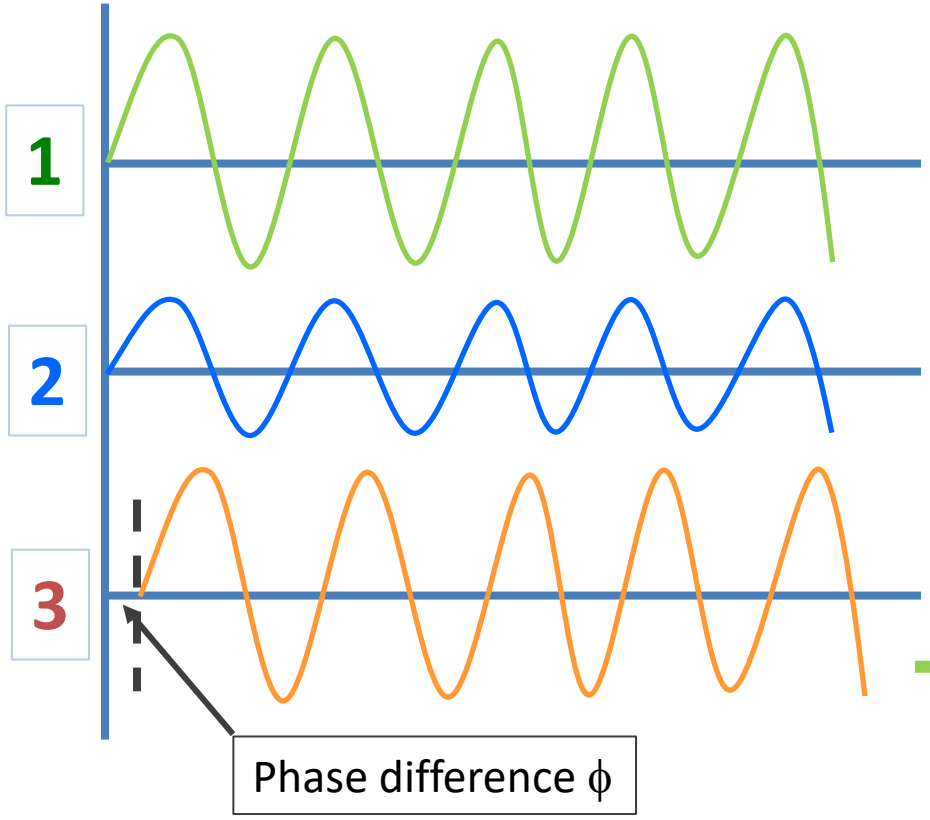

Adding vectors

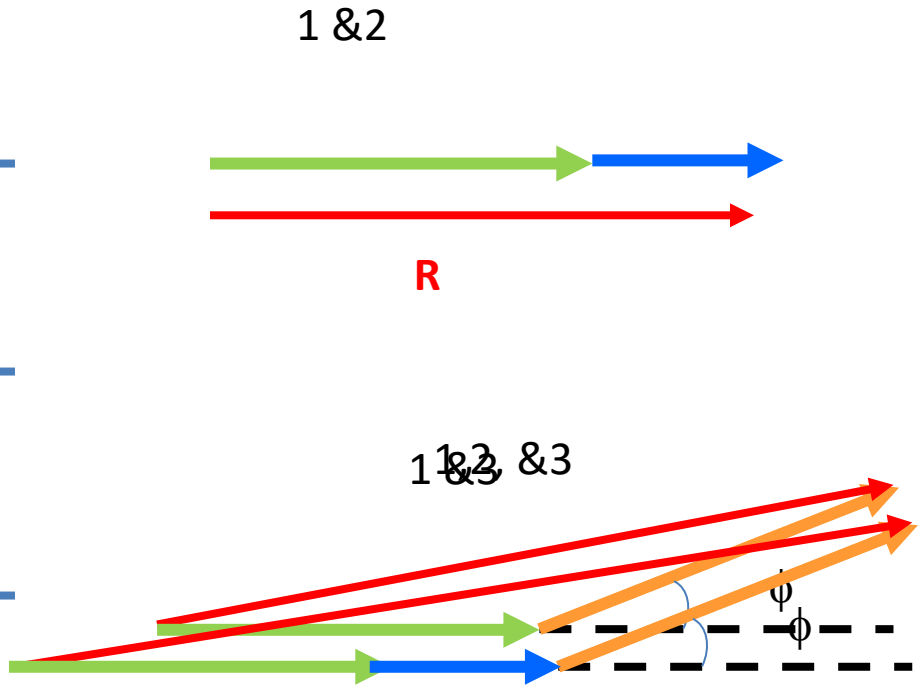

Amplitude of the wave ~ Magnitude or length of the vector
Phase of the wave ~ Direction of the vector

The resultant Vector (R) is the resultant Amplitude

Book1 - Microsoft Excel

Chart Tools

File | Home | Insert | Page Layout | Formulas | Data | Review | View | Add-Ins | Design | Layout | Format

Change Chart Type | Save As Template | Type | Switch Row/Column | Select Data | Data | Chart Layouts | Chart Styles | Move Chart | Location

Chart 1

	A	B	C	D	E	F	G	H
1								
2		t	I(t)	cos(2pif)	sin(2pif)		i(t)Cos(2pif)	i(t)*sin(2*pi*f)
3		1	0.882497	0.923879659	0.382683126		0.815320938	0.337716673
4		2	0.778801	0.70710725	0.707106312		0.55069568	0.55069495
5		3	0.687289	0.382684352	0.923879152		0.263014852	0.634972236
6		4	0.606531	1.32679E-06	1		8.04742E-07	0.60653066
7		5	0.535261	-0.3826819	0.923880167		-0.204834861	0.494517418
8		6	0.472367	-0.707105374	0.707108188		-0.334012928	0.334014257
9		7	0.416862	-0.923878644	0.382685578		-0.385129917	0.159527083
10		8	0.367879	-1	2.65359E-06		-0.367879441	9.76201E-07
11		9	0.324652	-0.923880675	-0.382680674		-0.299940141	-0.124238225
12		10	0.286505	-0.707109127	-0.707104436		-0.202590157	-0.202588813
13		11	0.25284	-0.382686803	-0.923878136		-0.096758377	-0.233592975
14		12	0.22313	-3.98038E-06	-1		-8.88144E-07	-0.22313016
15		13	0.196912	0.382679449	-0.923881183		0.075354051	-0.181922991
16		14	0.173774	0.707103498	-0.707110065		0.122876163	-0.122877304
17		15	0.153355	0.923877628	-0.382688029		0.141681223	-0.05868711
18		16	0.135335	1	-5.30718E-06		0.135335283	-7.18249E-07
19								
20		Sum	6.49399				0.213132286	1.970935956
21						g and s	0.032819929	0.303501541

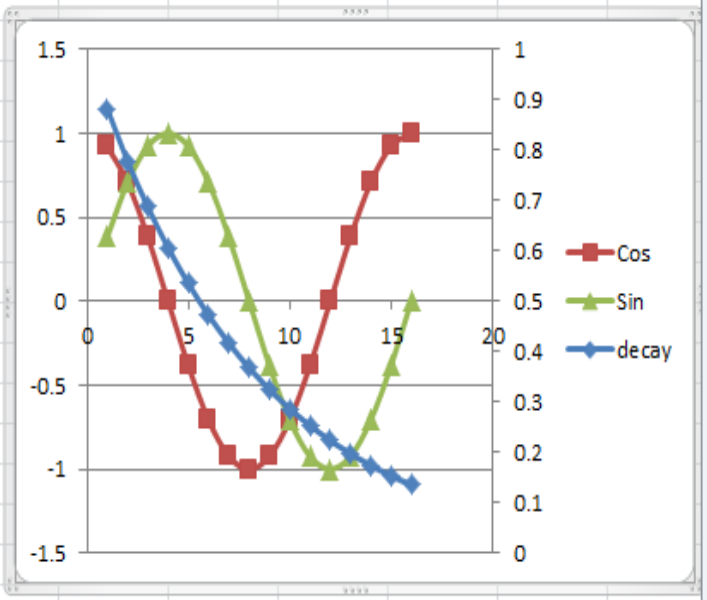

Sheet1 | Sheet2 | Sheet3

Ready

100%

The algebra of phasors: A fit free method

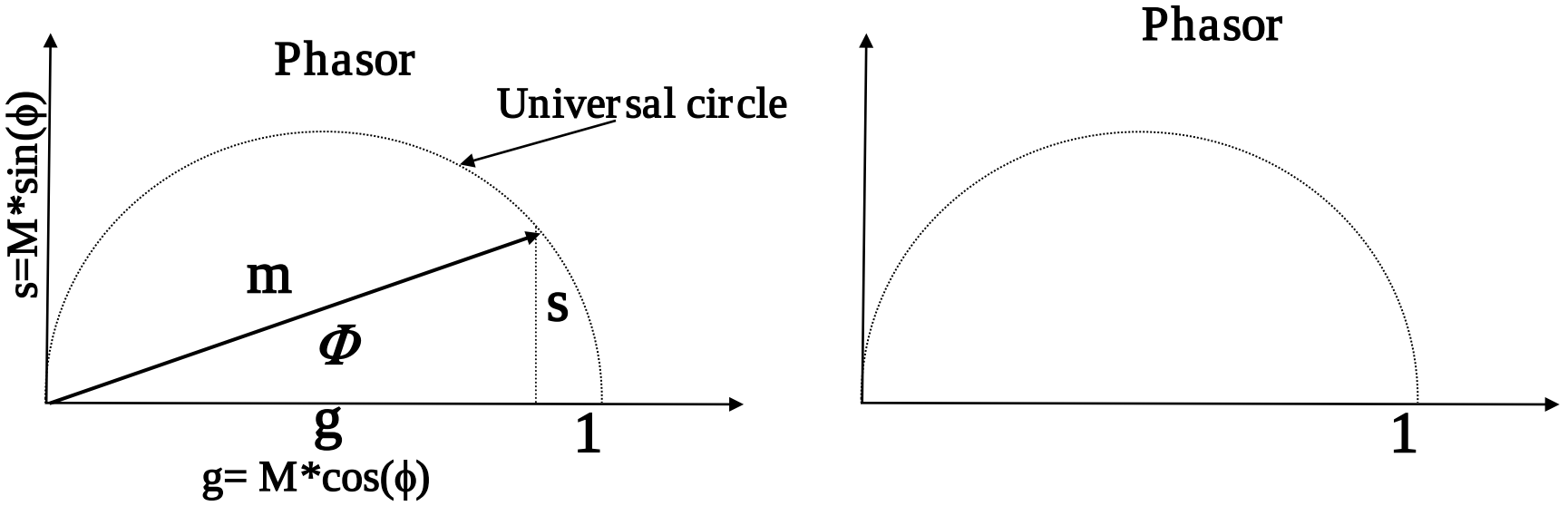

Simple rules to the Phasor plot:

1) All single exponential lifetimes lie on the “universal circle”
2) Multi-exponential lifetimes are a linear combination of their components
3) The ratio of the linear combination determines the fraction of the components

The algebra of phasors: A fit free method

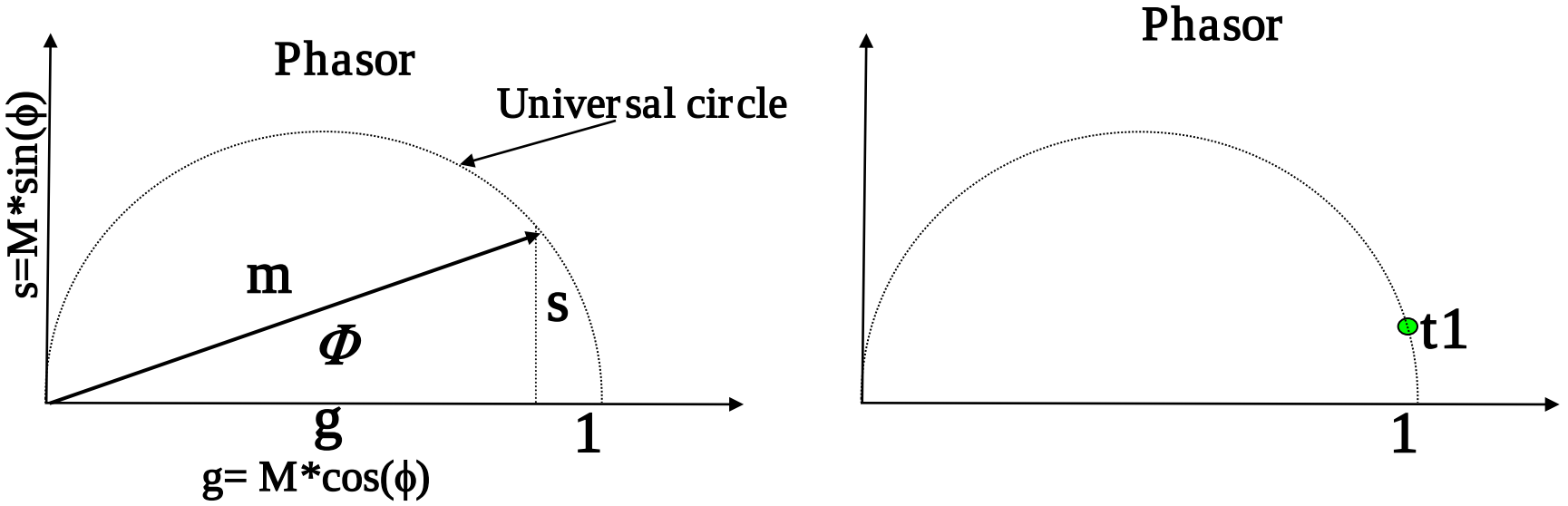

Simple rules to the Phasor plot:

1) All single exponential lifetimes lie on the “universal circle”
2) Multi-exponential lifetimes are a linear combination of their components
3) The ratio of the linear combination determines the fraction of the components

The algebra of phasors: A fit free method

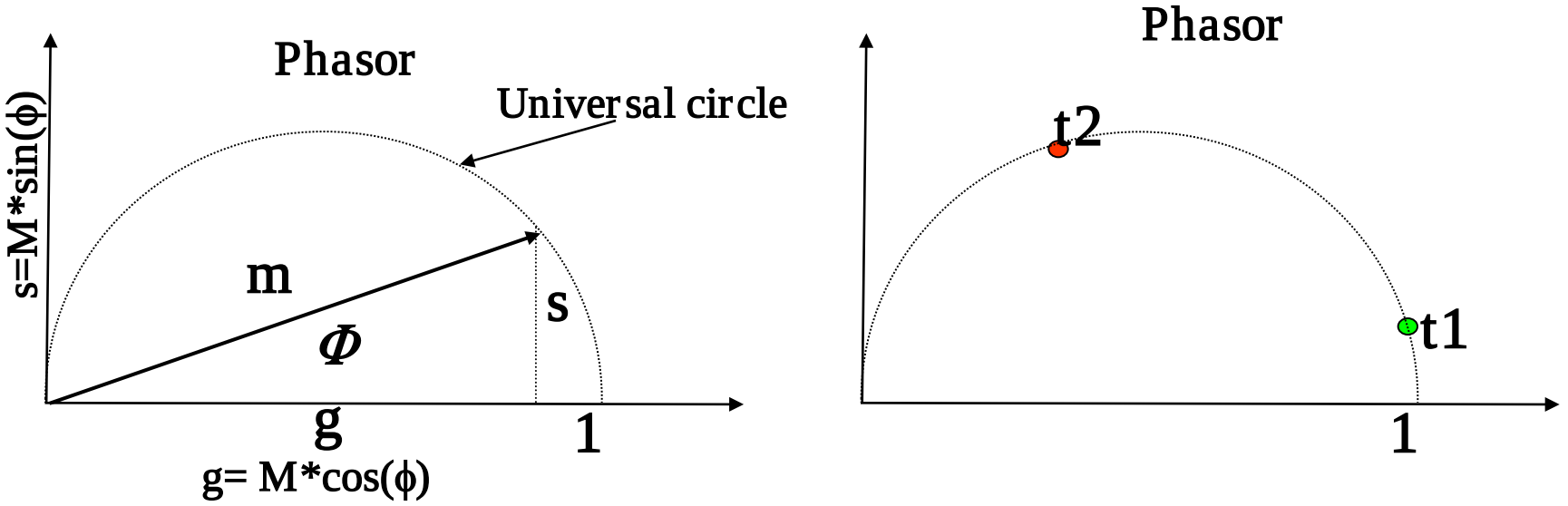

Simple rules to the Phasor plot:

1) All single exponential lifetimes lie on the “universal circle”
2) Multi-exponential lifetimes are a linear combination of their components
3) The ratio of the linear combination determines the fraction of the components

The algebra of phasors: A fit free method

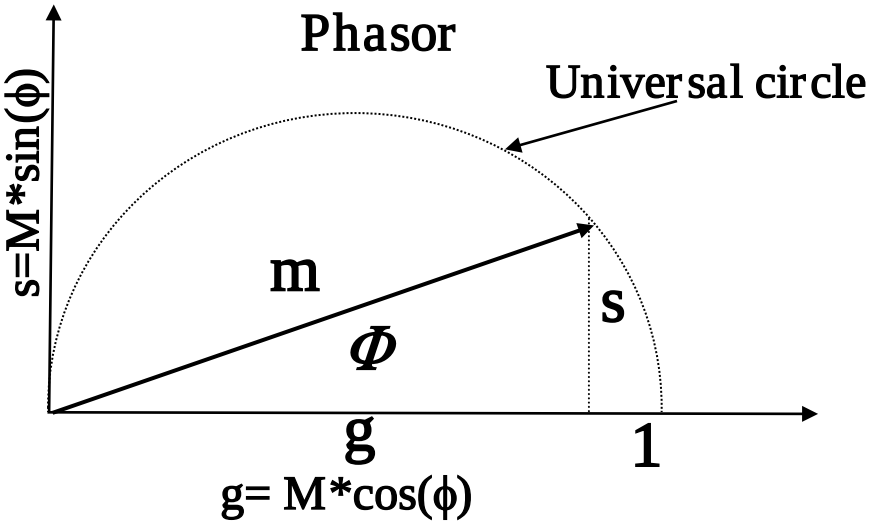

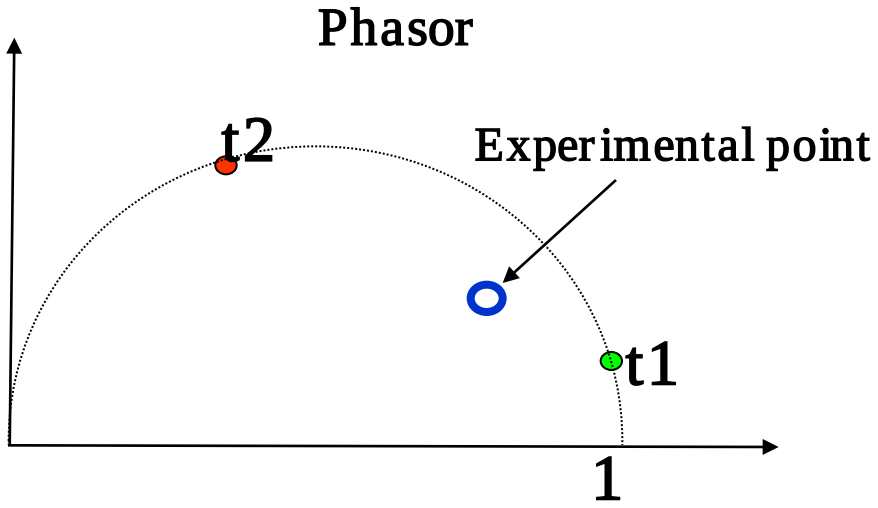

Simple rules to the Phasor plot:

1) All single exponential lifetimes lie on the “universal circle”
2) Multi-exponential lifetimes are a linear combination of their components
3) The ratio of the linear combination determines the fraction of the components

The algebra of phasors: A fit free method

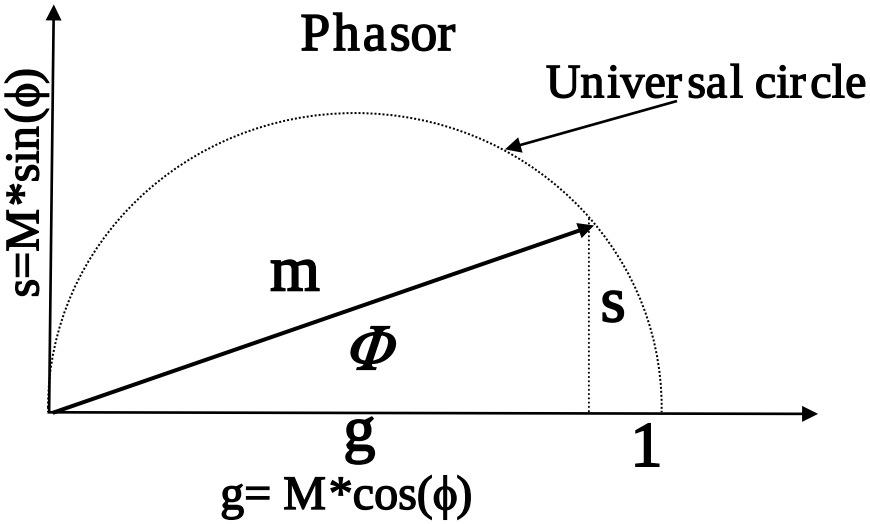

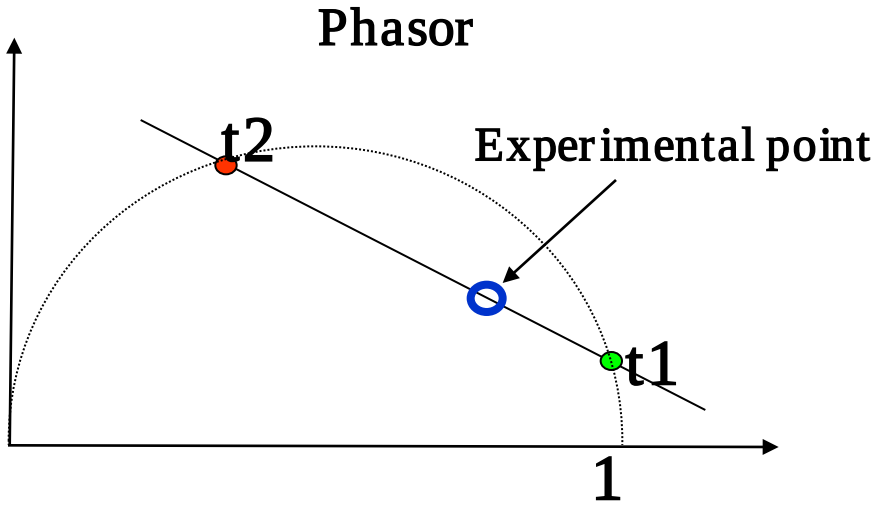

Simple rules to the Phasor plot:

1) All single exponential lifetimes lie on the “universal circle”
2) Multi-exponential lifetimes are a linear combination of their components
3) The ratio of the linear combination determines the fraction of the components

The algebra of phasors: A fit free method

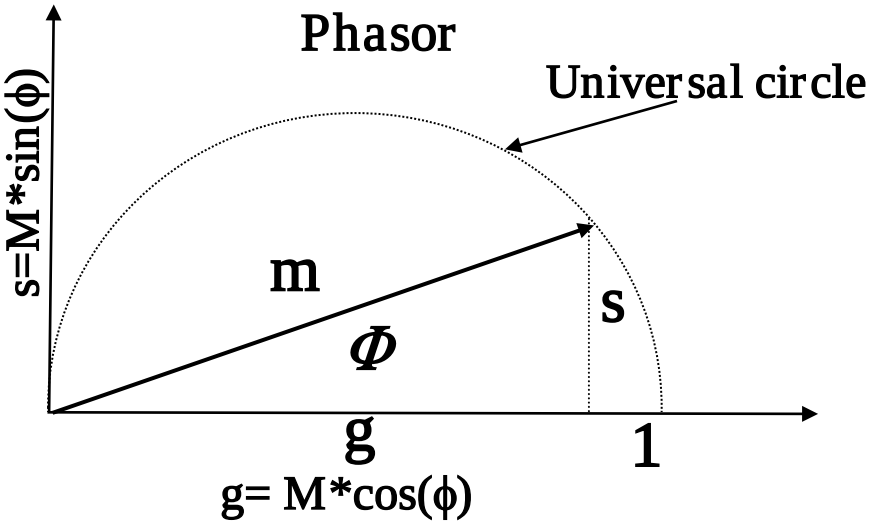

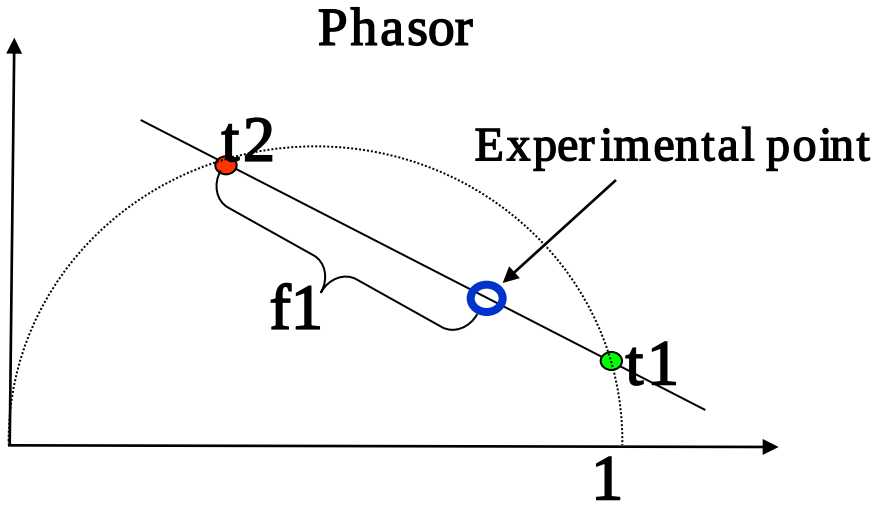

Simple rules to the Phasor plot:

1) All single exponential lifetimes lie on the “universal circle”
2) Multi-exponential lifetimes are a linear combination of their components
3) The ratio of the linear combination determines the fraction of the components

The algebra of phasors: A fit free method

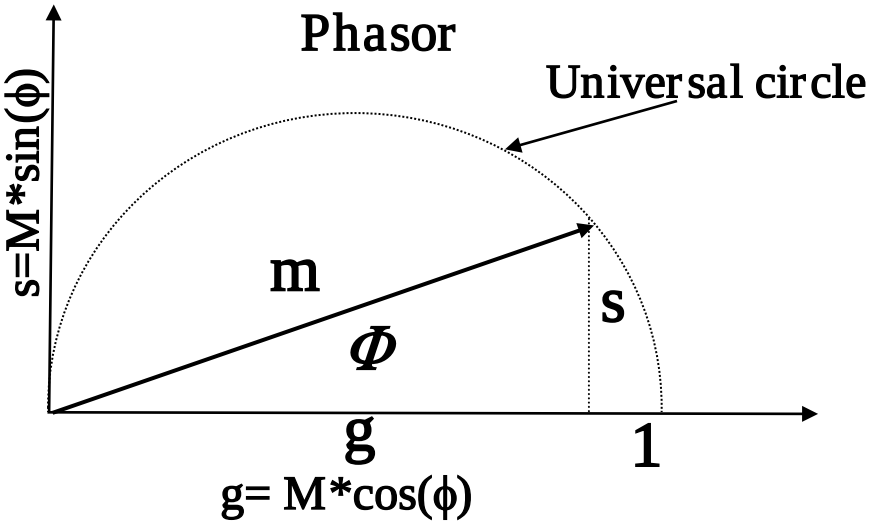

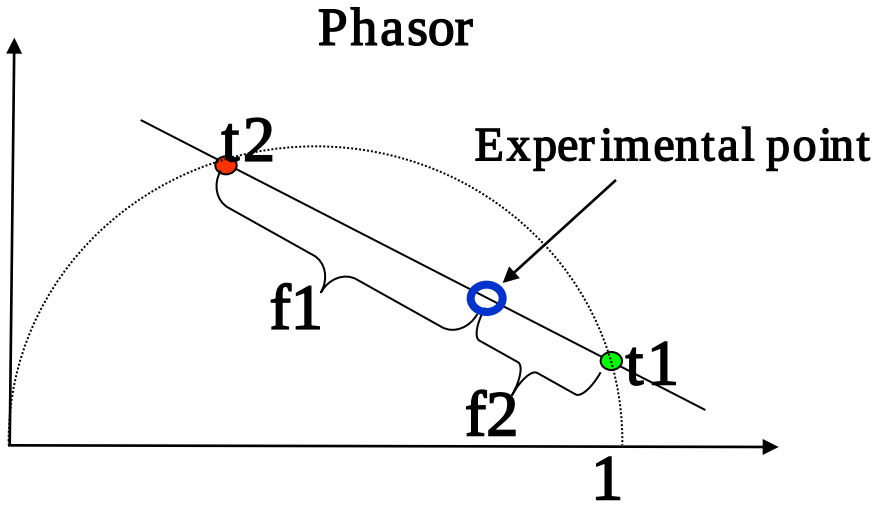

Simple rules to the Phasor plot:

1) All single exponential lifetimes lie on the “universal circle”
2) Multi-exponential lifetimes are a linear combination of their components
3) The ratio of the linear combination determines the fraction of the components

Phasor approach quickly reveals %Bound NADH

Phasors allow us to visualize data easily and efficiently, in our case the free to bound ratios of NADH.

* Each phasor represents the lifetime data for one pixel from the observation.
* Lifetimes are represented as points, called phasors, on the diagram.

Each pixel on the acquired image is converted through Fourier Transform to create coordinates in phasor space.

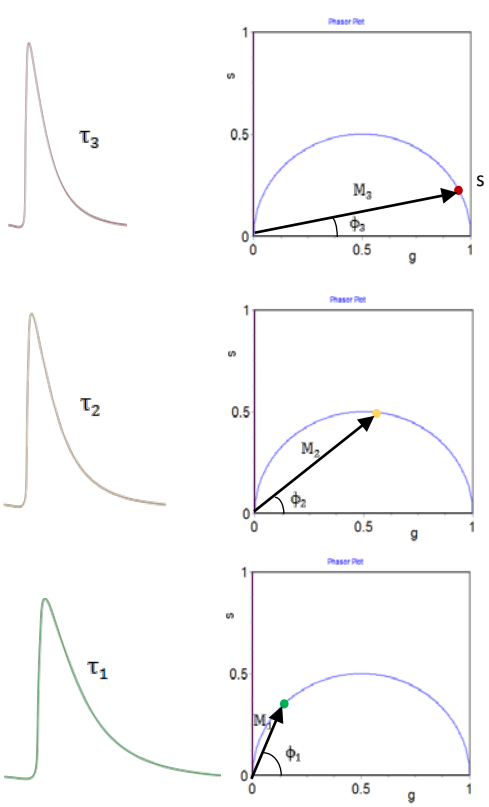

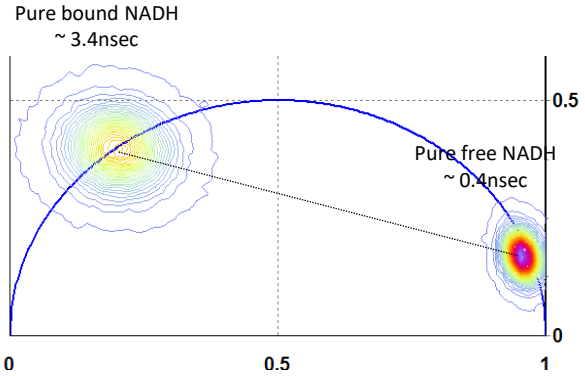

Law of linear addition of phasors:

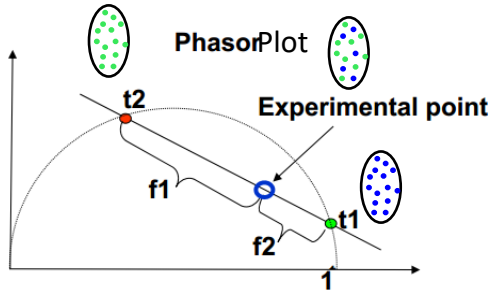

$$\text{Fraction of Bound NADH in Experimental Point} = \frac{f_2}{f_1 + f_2}$$

Digman M.A. et al Biophys J. 2008; 94(2): L14-16. PMC2157251

Phasor Fingerprint of pure chemical species….

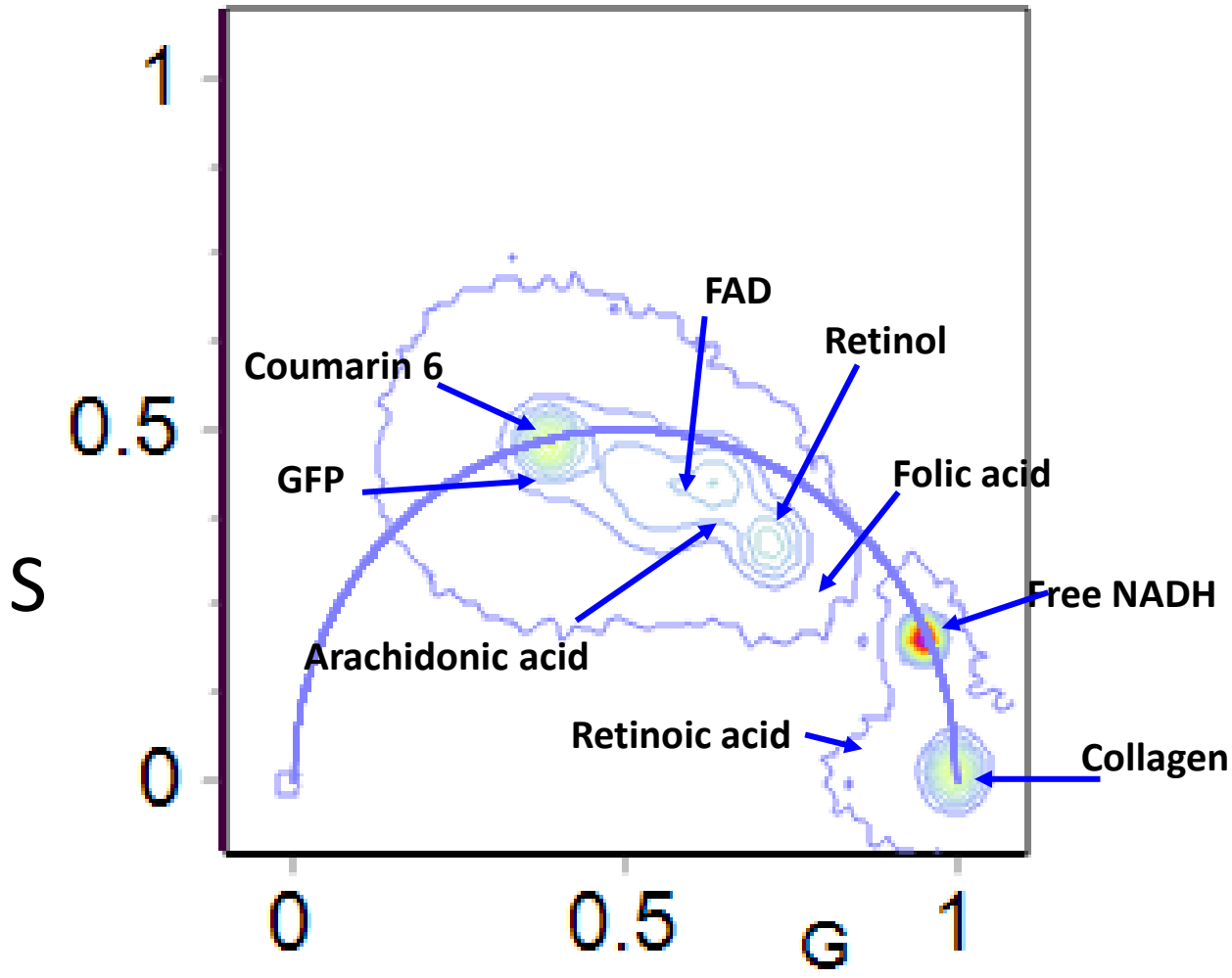

Metabolic Trajectory in the Phasor Plot

Free/bound NADH gradients associated with:

- Glycolysis/oxidative phosphorylation
- Oxidative stress
- cell proliferation
- differentiation
- Cancer

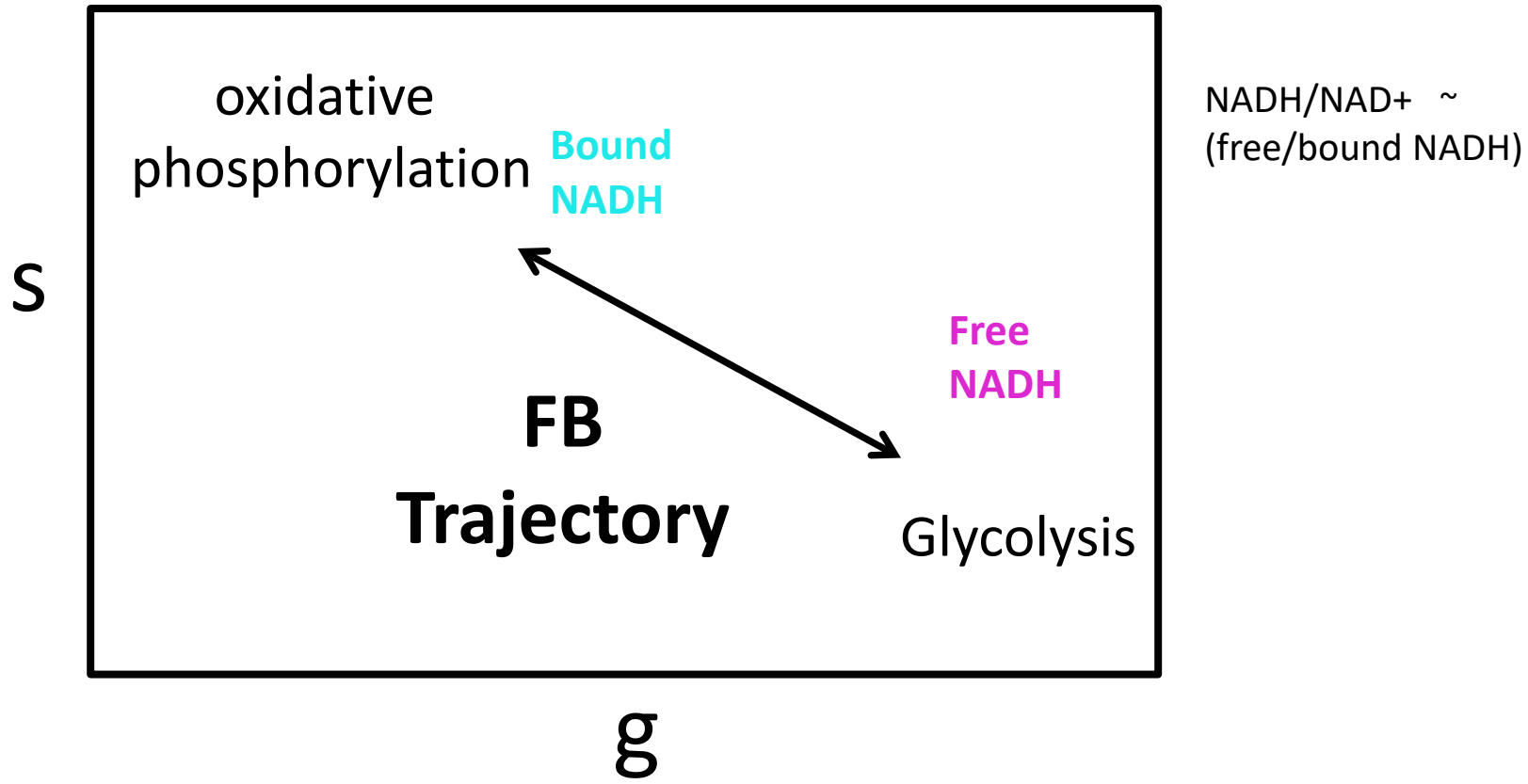

Linear combination of free and bound NADH

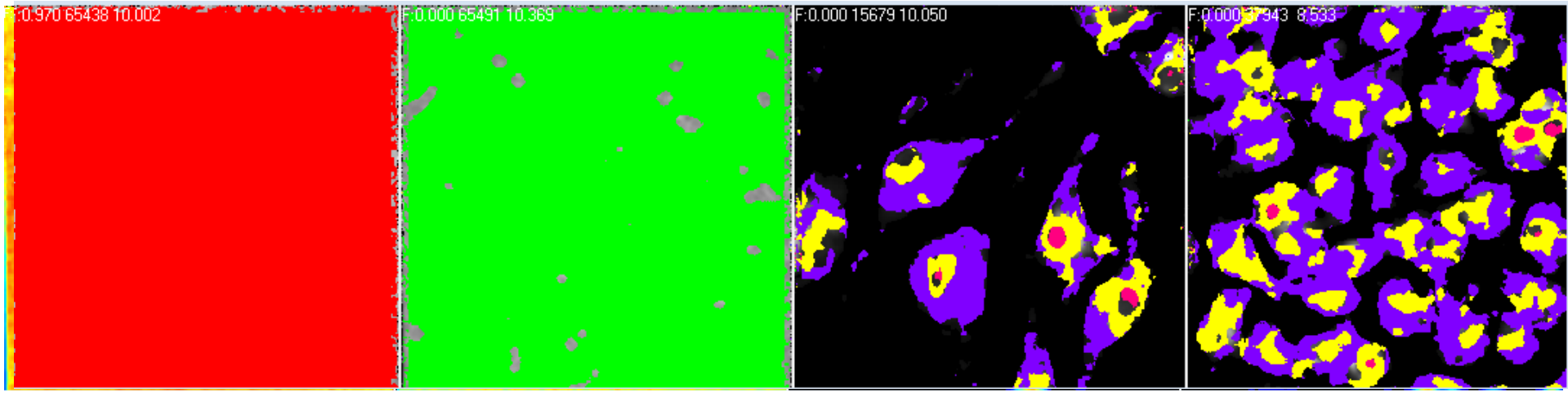

Free NADH

Bound NADH to LDH

M0 macrophages on glass

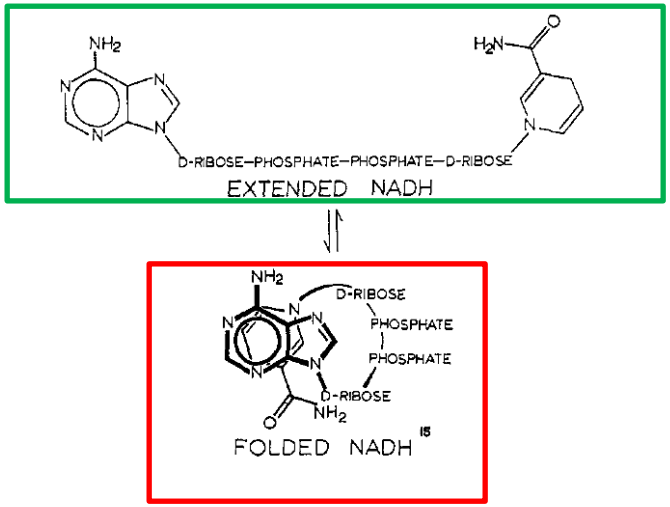

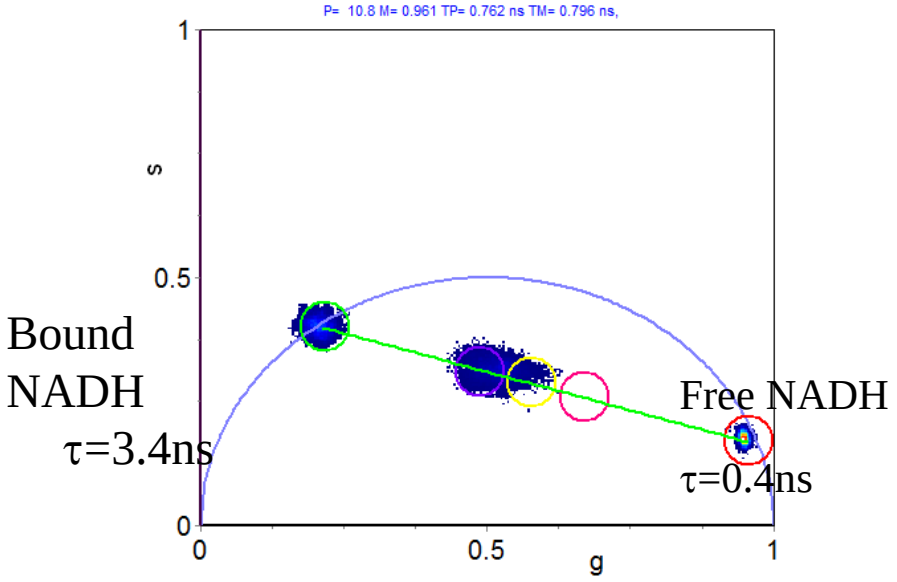

Hull, R. V., et al. *Biophys. Chem.* **90,** 9–16 (2001).

Why is NADH fluorescent while NAD+ is not?

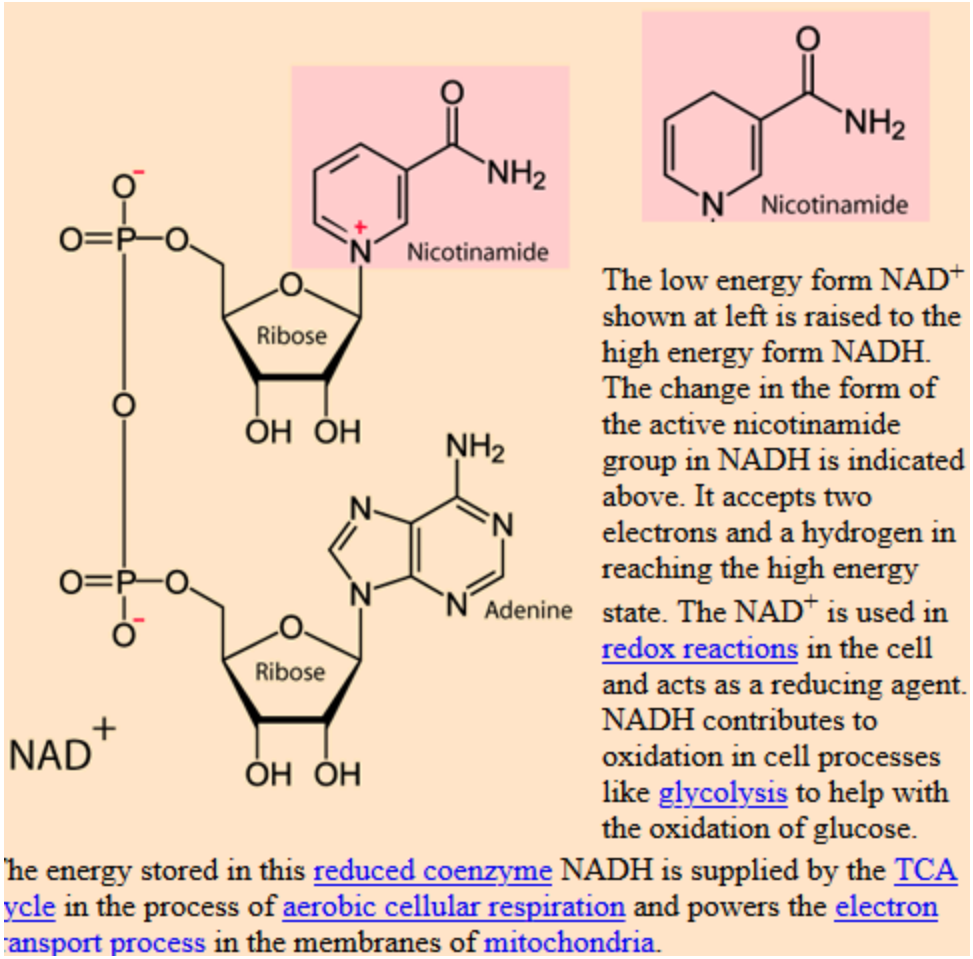

The low energy form NAD^+ shown at left is raised to the high energy form NADH. The change in the form of the active nicotinamide group in NADH is indicated above. It accepts two electrons and a hydrogen in reaching the high energy state. The NAD^+ is used in redox reactions in the cell and acts as a reducing agent. NADH contributes to oxidation in cell processes like glycolysis to help with the oxidation of glucose.

he energy stored in this reduced coenzyme NADH is supplied by the TCA ycle in the process of aerobic cellular respiration and powers the electron ransport process in the membranes of mitochondria.

http://hyperphysics.phy-astr.gsu.edu/hbase/Organic/nad.html

Phasor FLIM measurement of Free/Bound NADH in tissue to assess metabolism

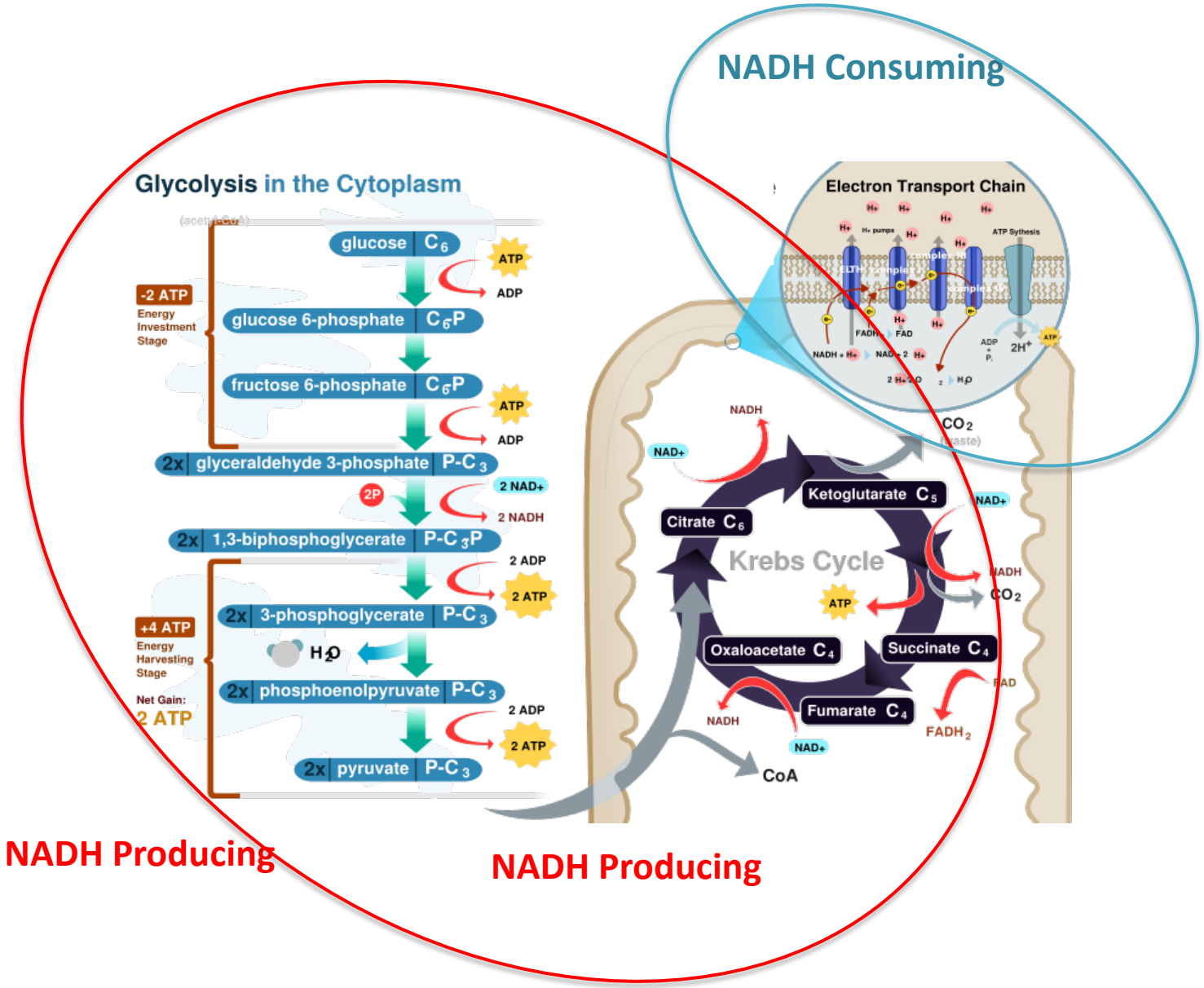

Metabolism in tissues

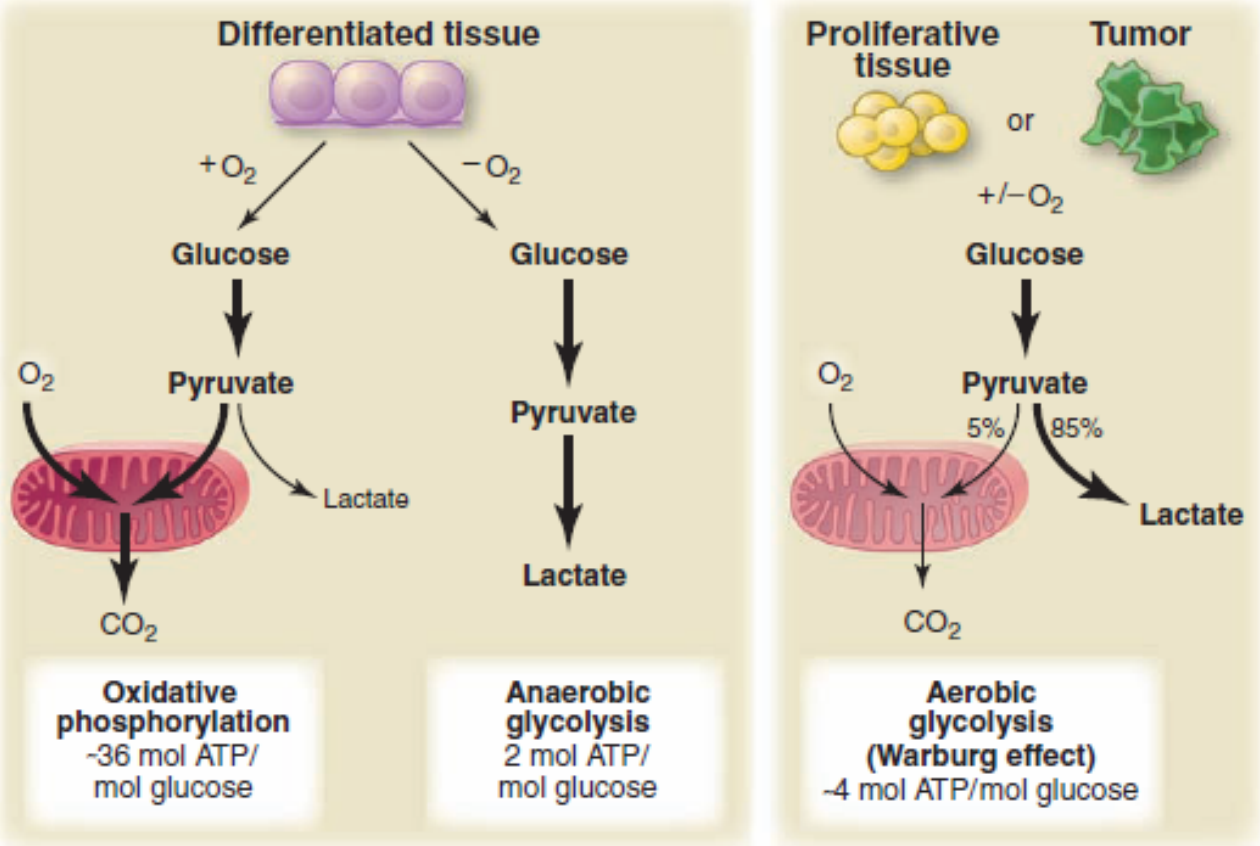

LOW NADH/NAD+
(LOW free/bound NADH)

HIGH NADH/NAD+
(**HIGH** free/bound NADH)

Cairns et al. Nature reviews Cancer 2011

Heiden, *et al. Science* 2009

Metabolic Trajectory

Oxidized NAD+/ Reduced NADH --> Free/bound NADH

Electron chain inhibition

Before

KCN

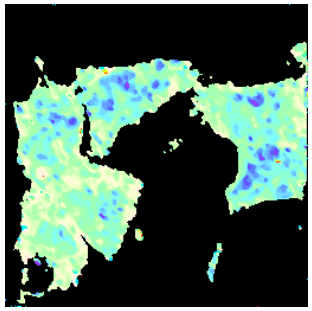

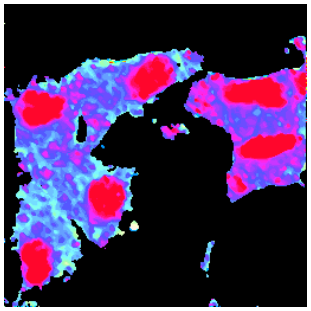

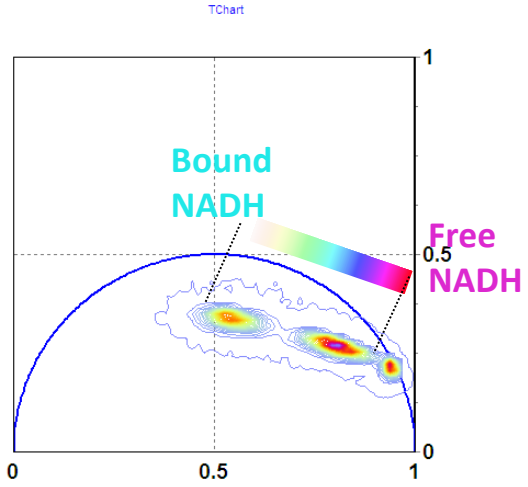

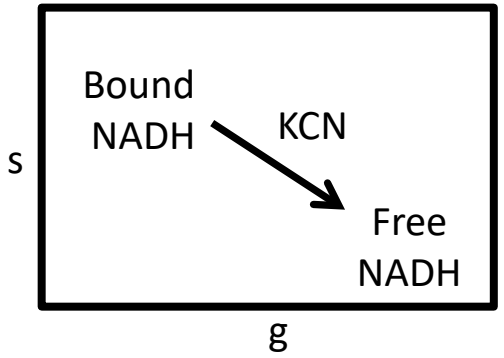

Oxidative stress

Before

H_2O_2

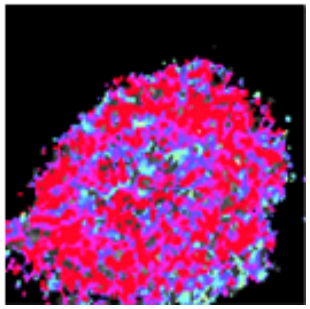

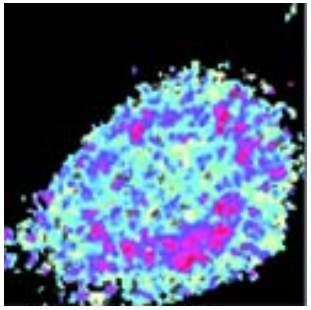

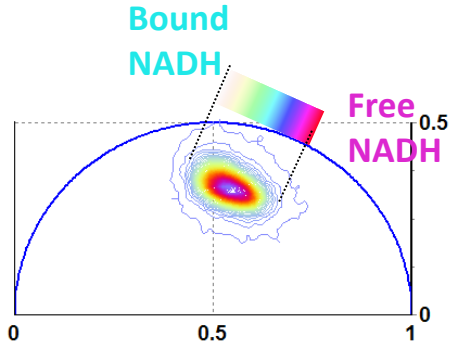

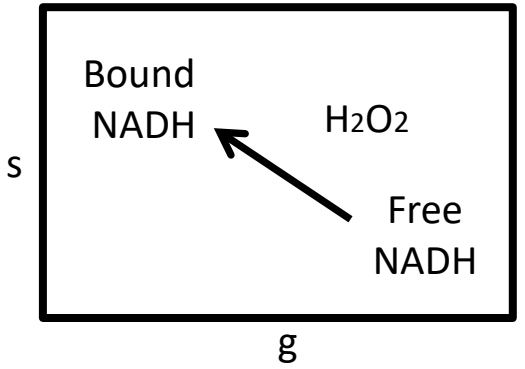

Metabolic Trajectory

glycolysis/ oxidative phosphorylation --> Free/bound NADH

Glucose uptake

4.5 mM glucose

22 mM glucose

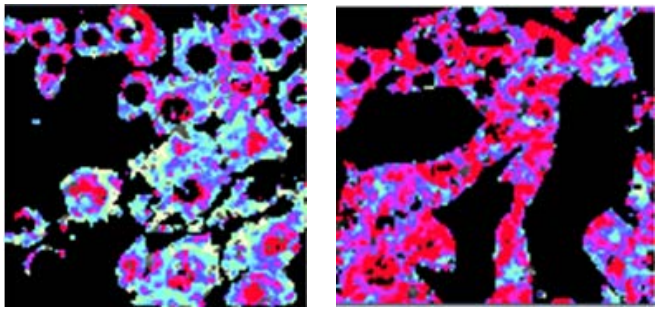

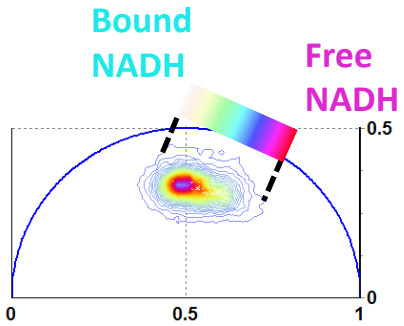

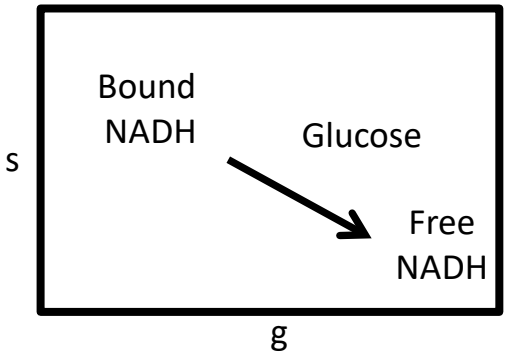

Glycolysis inhibition
Dichloroacetate (DCA)
metabolic-targeting cancer drug

control

DCA

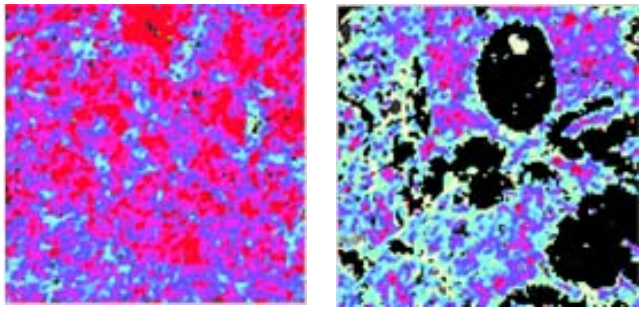

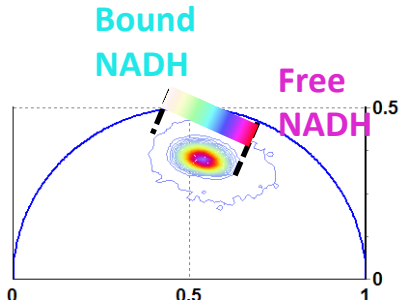

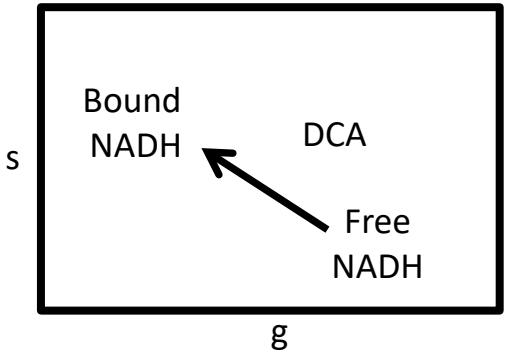

The Metabolic trajectory in aging and Alzheimer's Disease

Driving Biological Question:

- The Epigenetic Oxidative Redox Shift (EORS) theory of aging proposes that a sedentary low-energy state with aging triggers an oxidative shift and mitochondrial dysfunction* and further causes metabolic disturbances

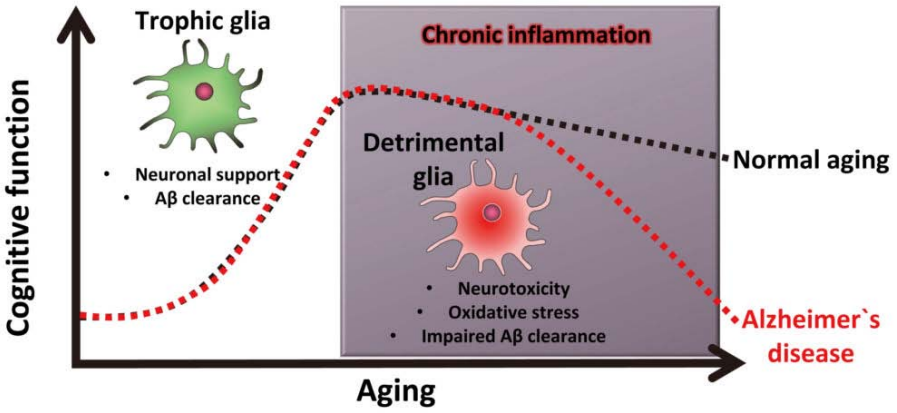

Aging is `associated with chronic inflammation, which has been identified as both a key contributor to the initiation and progression of Alzheimer`s disease

- <u>Our hypothesis:</u> free NADH in neurons from old mice is lower than the levels in young mice and even lower in neurons from the 3xTg-AD Alzheimer's disease (AD) mouse model

*due to the accumulation of free radical damage over time

Three alternative mechanisms for energy production that maintain NAD^+ levels for glycolysis and redox balance

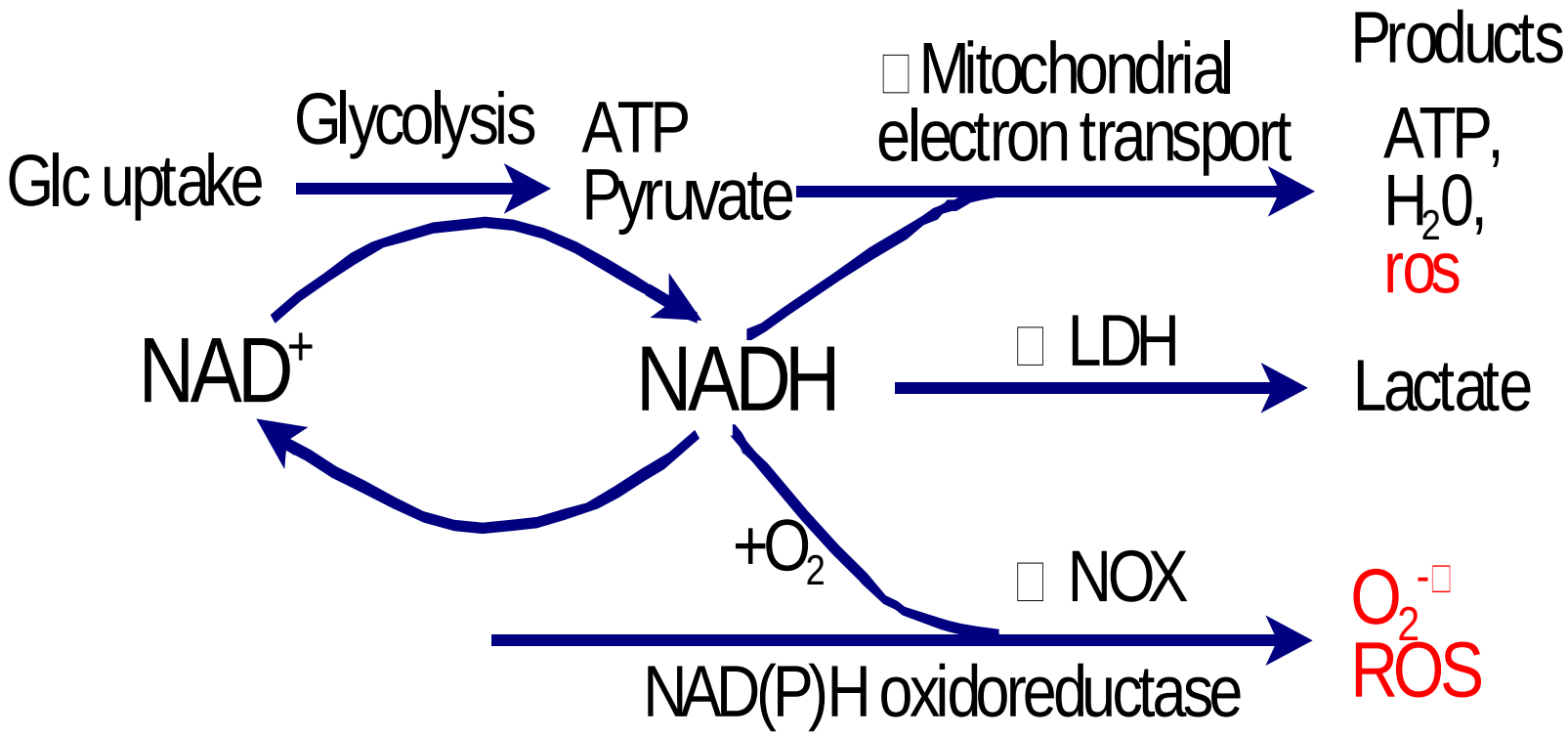

Brewer 2010

de Grey AD (1998) A mechanism proposed to explain the rise in oxidative stress during aging. J Anti-Aging Medicine 1:53-66.

Dilemmas of current aging theories

Aging Paradigm/Observations	**Impact**	**Dilemmas**
1**) Oxyradical damage** to macromolecules (Harman, 1952)	Cumulative cellular damage leads to organ failure, shortened life-span	Exercise extends lifespan but produces ROS (Powers SK 2008) Ignores insulin signaling SOD, catalase Xgenics(Perez VI 2009)
2) Genetic reductions in the insulin signaling path (Carter CS 2002) or **caloric restriction** (Weindruch R 2001)	Increased life-span, may decrease metabolism = “slower” rate of living (Pearl R 1928)	Metabolism actually increases (Westbrook R 2009) Ignores role of ROS
3) Both		Ignore healthy aging, energetics and ROS signaling vs. ROS inflammation

EORS, a vicious cycle of aging enforced by an **E**pigenetic **O**xidized **R**edox **S**hift unifies the free radical and insulin signaling theories

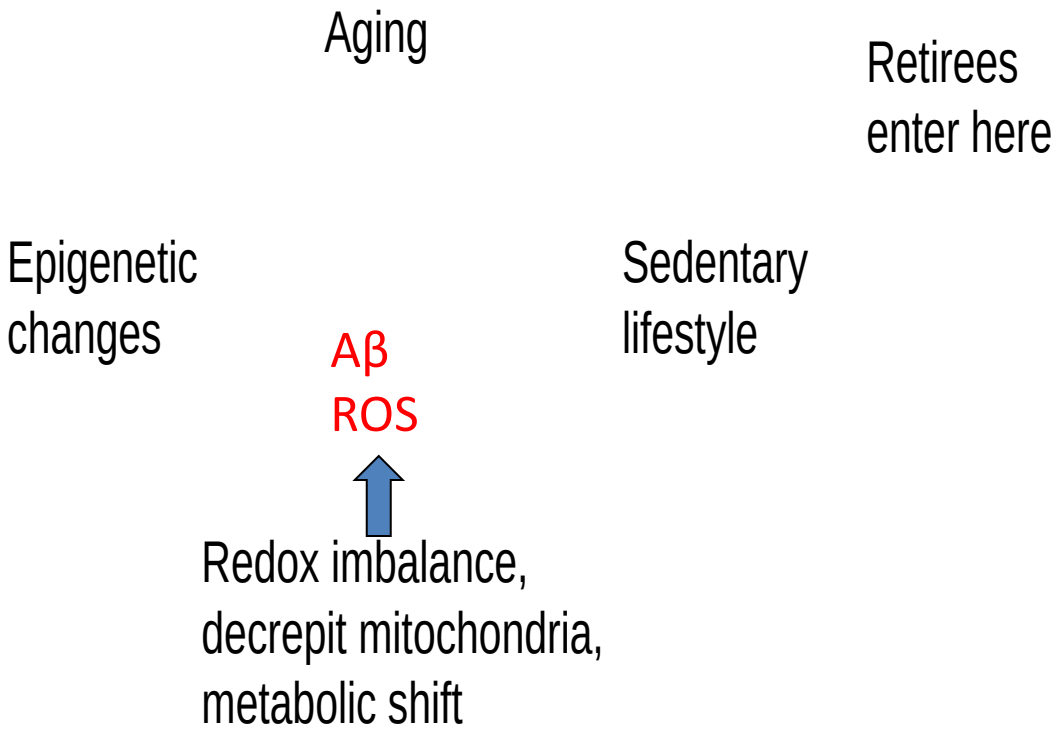

Brewer 2010

- Aging and AD share some common characteristics such as:
  - oxidative stress
  - mitochondrial impairment
  - bioenergetic deficits

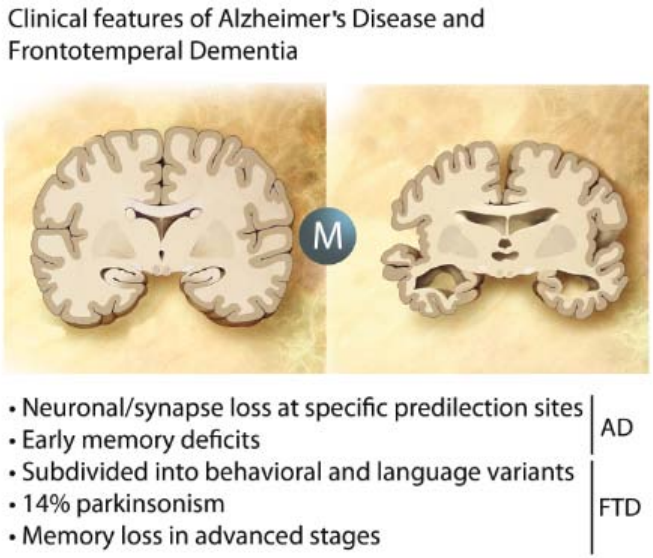

Histopathologically, AD is characterized by Aβ plaques & neurofibrillary lesions.

Aβ in the plaques is fibrillar.

The 3xTg-AD mouse model: combined Aβ plaque and NFT (neurofibrillary tangles) pathology

	Tau X	Aβ	Observations	References
A.	JNPL3 (P301L) 	Tg2576 ($Aβ^{sw}$) 	• 7x NFT induction • No increase in Aβ pathology	Lewis et al., Science 2001
B.	pR5 (P301L) 	i.c. Aβ 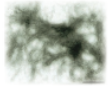	• 5x NFT induction	Gotz et al., Science 2001
C.	3xtg-AD (P301L/APP^{sw}/$PSEN1^{M146/-}$ ki) 		• NFTs and plaques preceded by synaptic/LTP deficits • Correlated with intra-neuronal Aβ • Blocking Aβ delays onset/progression of tau pathology	Oddo et al., Neuron 2003; Oddo et al., J Neurosci 2008; Billings et al., Neuron 2005

- Decreased mitochondrial numeric density (number of mitochondria/μm 3 of cytoplasm) in in 10-month-old mice but the volume and average length increased
- decreased mitochondrial number with age in the hippocampus along with abnormal mitochondrial morphology with elongation, swelling and disorganized cristae
- decline in the motility of mitochondria in the due to changes in Drp1levels for fission

*these mitochondrial structural changes reflect functional deficits of free NADH as a bioenergetic substrate for oxidative phosphorylation (OXPHOS) that initiates a vicious cycle involving redox imbalance, energetic shortage, and mitochondrial dysfunction.

Image segmentation and phasor compartment average:

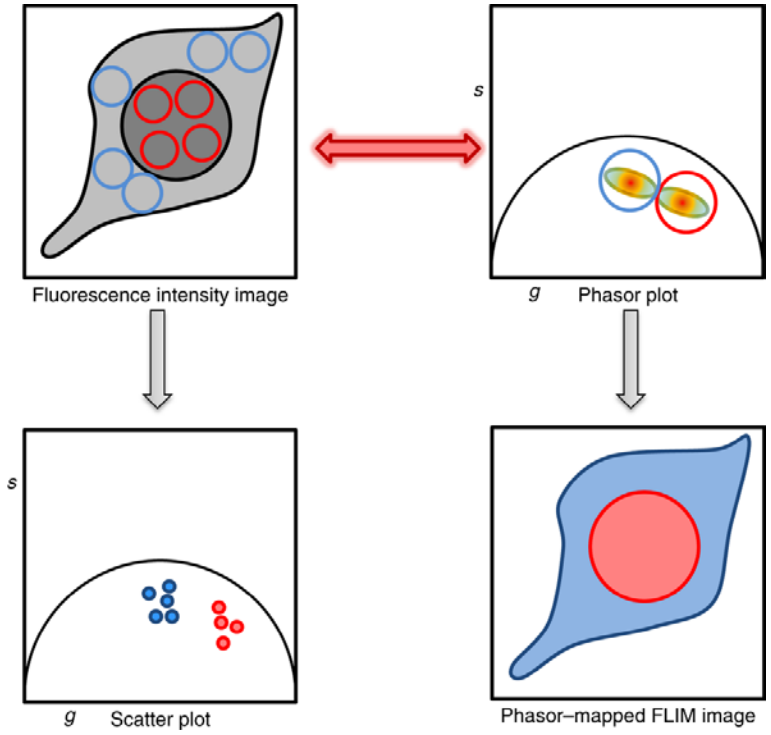

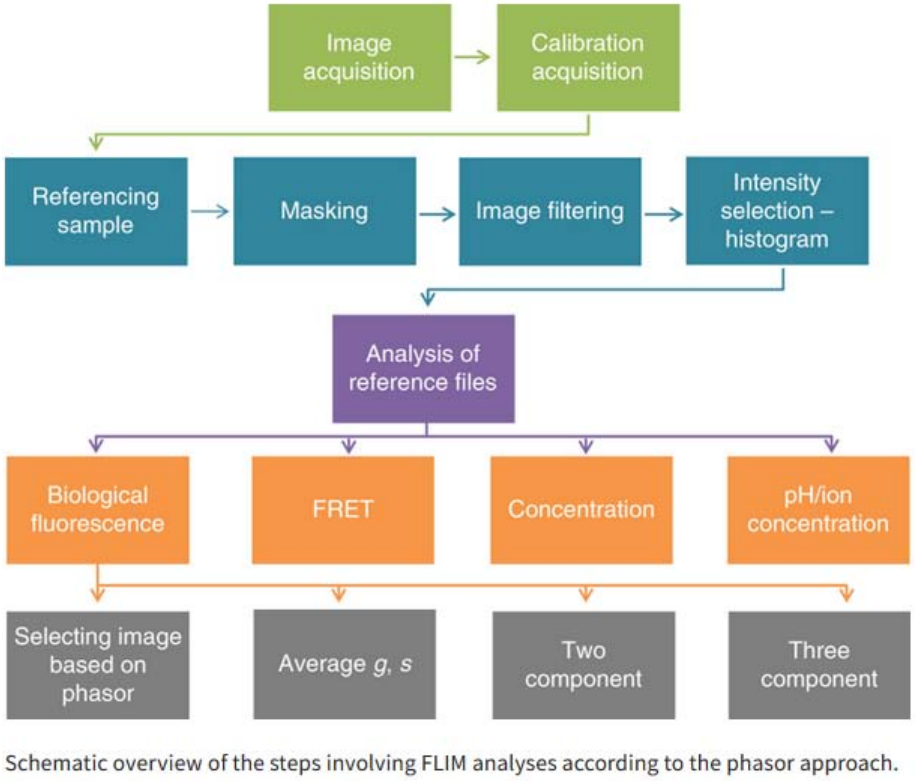

Schematic overview of the steps involving FLIM analyses according to the phasor approach.

Fit-free analysis of fluorescence lifetime imaging data using the phasor approach
Ranjit et al, Nature Protocols **3**, pages1979–2004 (2018)

AD genotype shows lower free NADH fraction than the corresponding compartment levels of *NTg control* mice neurons.

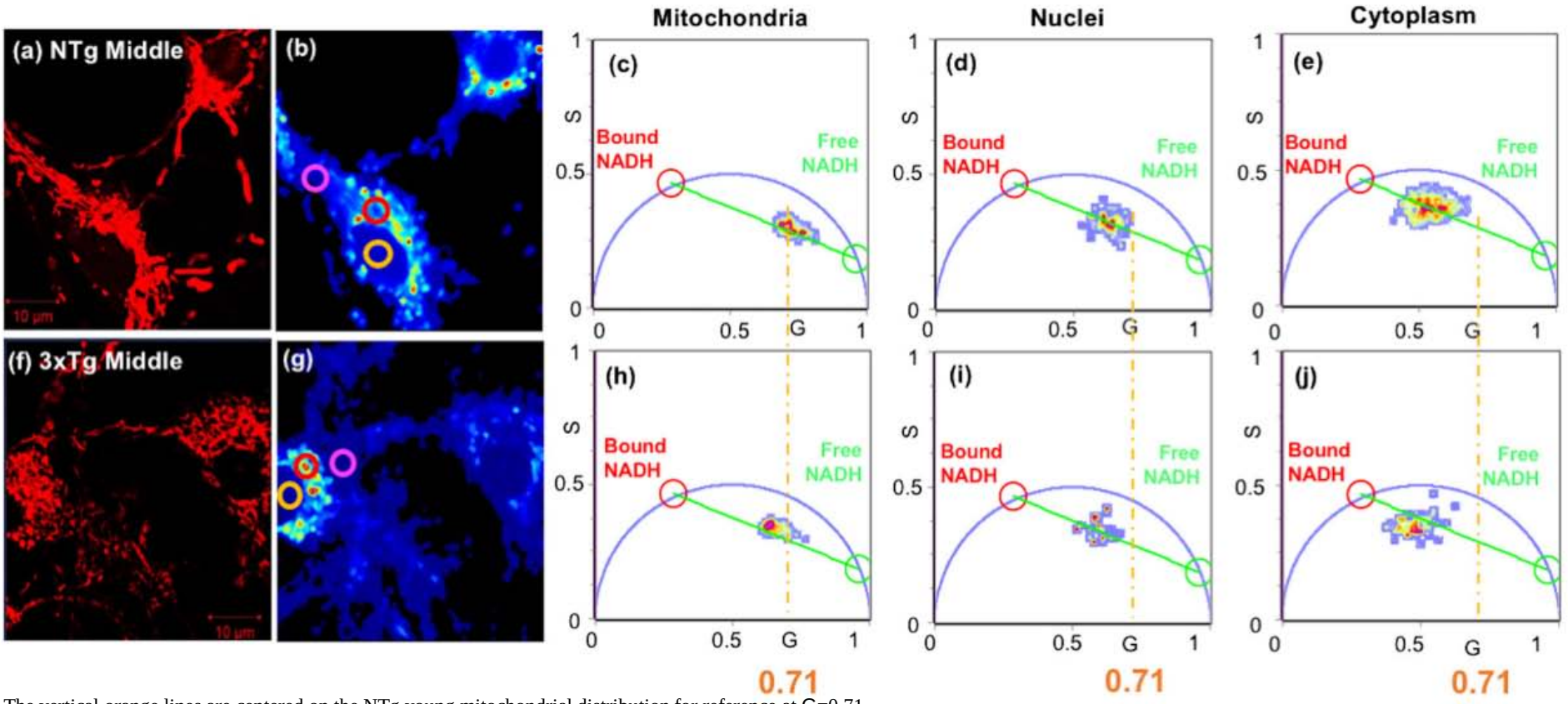

The vertical orange lines are centered on the NTg young mitochondrial distribution for reference at G=0.71

Free NADH highest in mitochondria > nuclei > cytoplasm

Free NADH levels lower in 3xTg-AD genotype neurons than NTg

Dong Y, **Digman MA**, Brewer GJ. Geroscience. 2019; 41(1): 51-67.

Aging promotes shifts toward more bound and less free NADH in NTg control and 3xTg-AD neurons

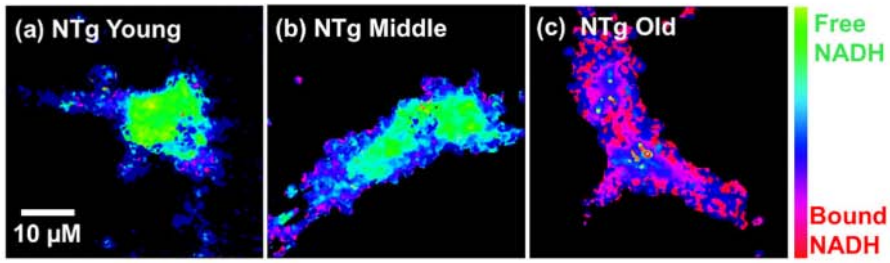

young (3–4 months old), middle ages (9–10 months old), and old ages (18, 21, 22, 23 months old)

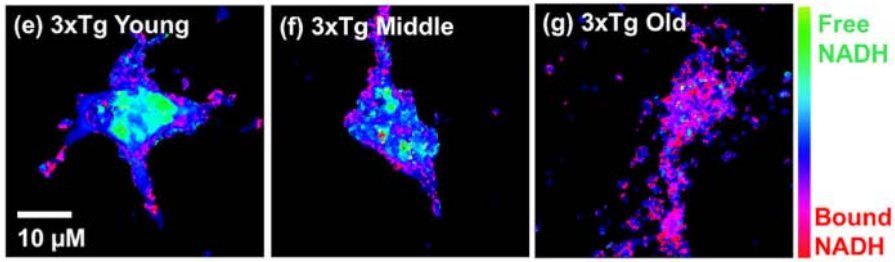

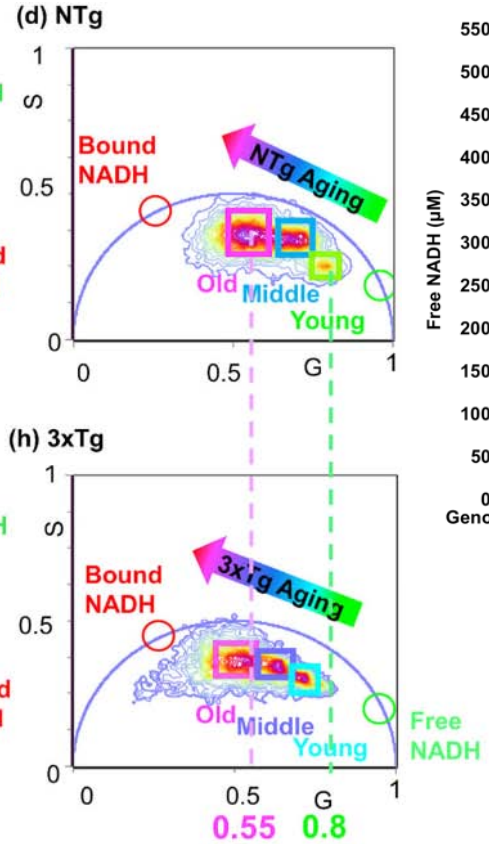

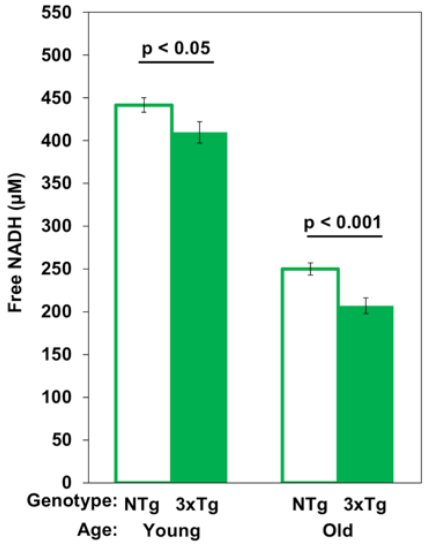

NTg 43% and 3xTg 50% drop in mitochondrials free NADH available for oxidative phosphorylation with aging

Dong Y, **Digman MA**, Brewer GJ. Geroscience. 2019; 41(1): 51-67.

Aging strongly drove a decline in the free NADH fractions in all subcellular compartments in both genotypes and both genders.

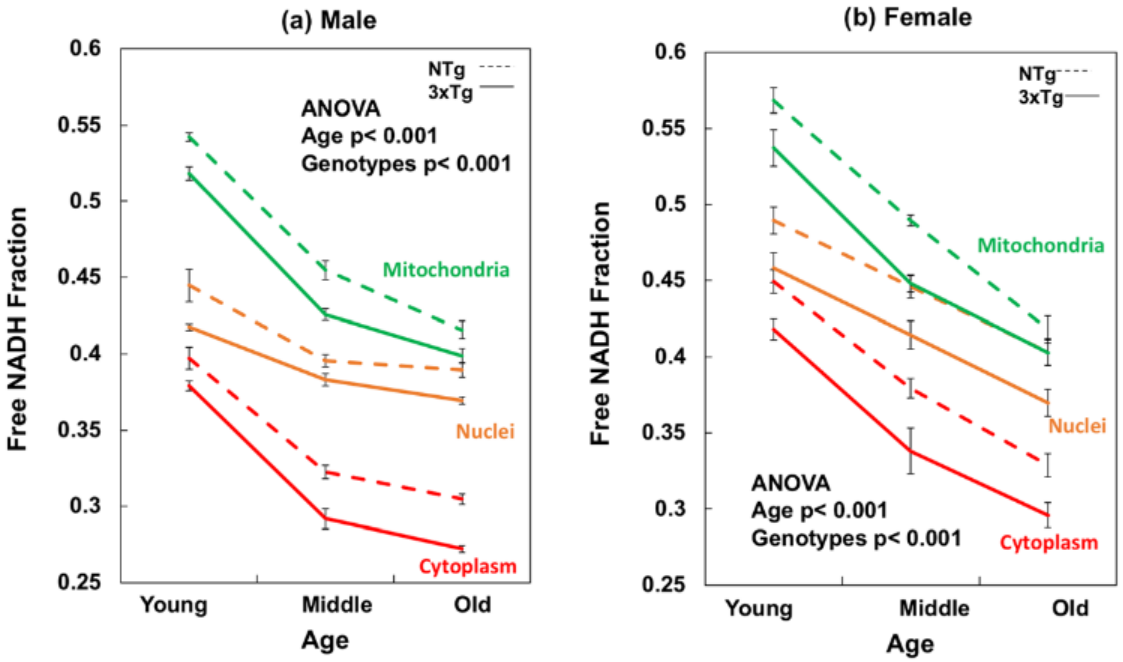

Mitochondria

- The relative order of compartmental free to bound NADH redox states was independent of age and genotype.
- Overall, the largest changes in free NADH were associated with age, then compartment, genotype, and gender
- The highest free NADH fraction in mitochondria suggests that mitochondria have the highest capacity for free NADH production compared to nuclei and cytoplasm.

Dong Y, **Digman MA**, Brewer GJ. Geroscience. 2019; 41(1): 51-67.

Aging depleted free NADH levels in all compartments of both genotypes: Free NADH fraction only 5-10% in male

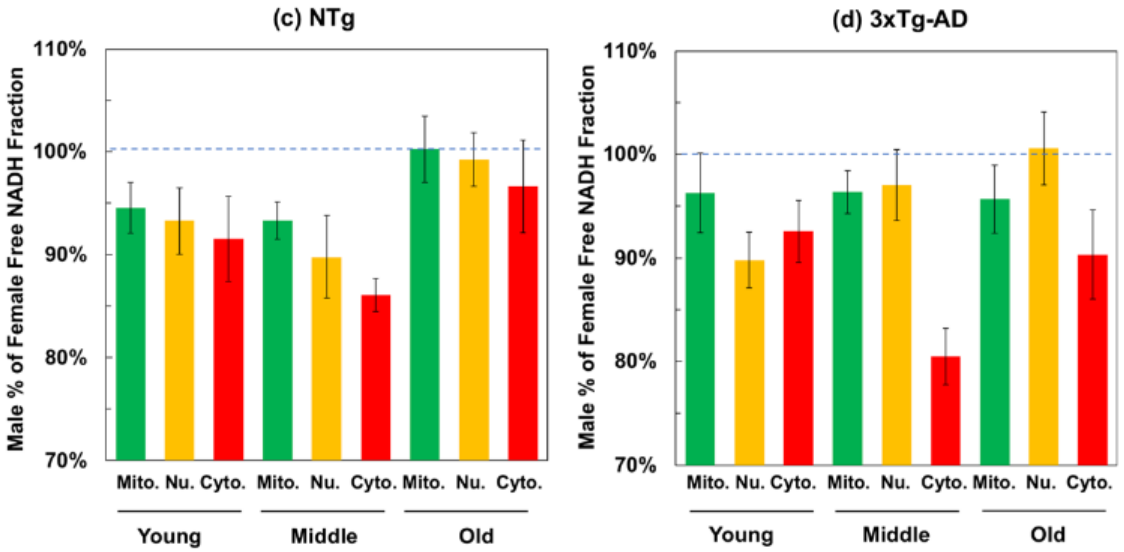

1) By gender: male neurons were lower in free NADH fraction than neurons at young and middle ages, but the multiple comparison results indicated no significant differences in old ages between female and male neurons

2) There is gender differences in the young and middle age of all compartments, but no significant gender differences at old ages. This suggests that higher reductive capacity in females than males is gradually lost in old age.

Dong Y, **Digman MA**, Brewer GJ. Geroscience. 2019; 41(1): 51-67.

Summary and Conclusions

Age- and AD-dependent decline in free NADH

- The lower free NADH with age and further decrease with AD genetic load can be due to a decrease in enzymes concentration which produce NADH in the TCA cycle. AD cells are known to have declines in these dehydrogenases that would lead to lower free NADH production in mitochondria.
- As compensatory effects, pathways may redirect fluxes to replenish the decreasing NADH levels. Nicotinamide nucleotide transhydrogenase reverses the direction of reaction to generate more NADH at the cost of NADPH. This begins a vicious cycle because NADPH is needed to regenerate GSH as the major redox buffer, when GSH levels are decreased by age-associated oxidative stress. Age- and AD-related oxidative shifts stimulate up-regulation of glycolytic pathway to feed the NADH & energetic demand.
- We found that levels of free NADH in male neurons were significantly lower than those of age and genotype matched female mouse brains, particularly in the cytoplasmic compartment. This protective effect of higher free NADH levels in female neurons appears to lessen with age, ending in similar free NADH levels in old neurons of female and male.

GeroScience (2019) 41:51–67
https://doi.org/10.1007/s11357-019-00052-8

CrossMark

ORIGINAL ARTICLE

Age- and AD-related redox state of NADH in subcellular compartments by fluorescence lifetime imaging microscopy

Yue Dong · Michelle A. Digman · Gregory J. Brewer

Future Directions

1. How could age-related deficits in intracellular NADH be assessed in the elderly non-Invasively and cost-effectively? (red blood cells transdermal?)

2. How could intracellular NADH be elevated orally and can they be quantitatively controlled?

3. Can elevated intracellular NADH slow progression of AD, stall conversion from MCI to AD or improve cognitive function in MCI subjects?

4. Will supplementary intracellular NADH rescue the observed age- and AD-related metabolic shifts implicated in AD?

Metabolism During Mouse Embryo Development

1. From the 2-8 cells stage metabolism is pyruvate based (oxidative phosphorylation).

2. Hexokinase is inhibited in the first stage of embryo development then around the morula stage there is an increase in glucose uptake and increase activity of hexokinase thereby making glycolysis the major source of energy production

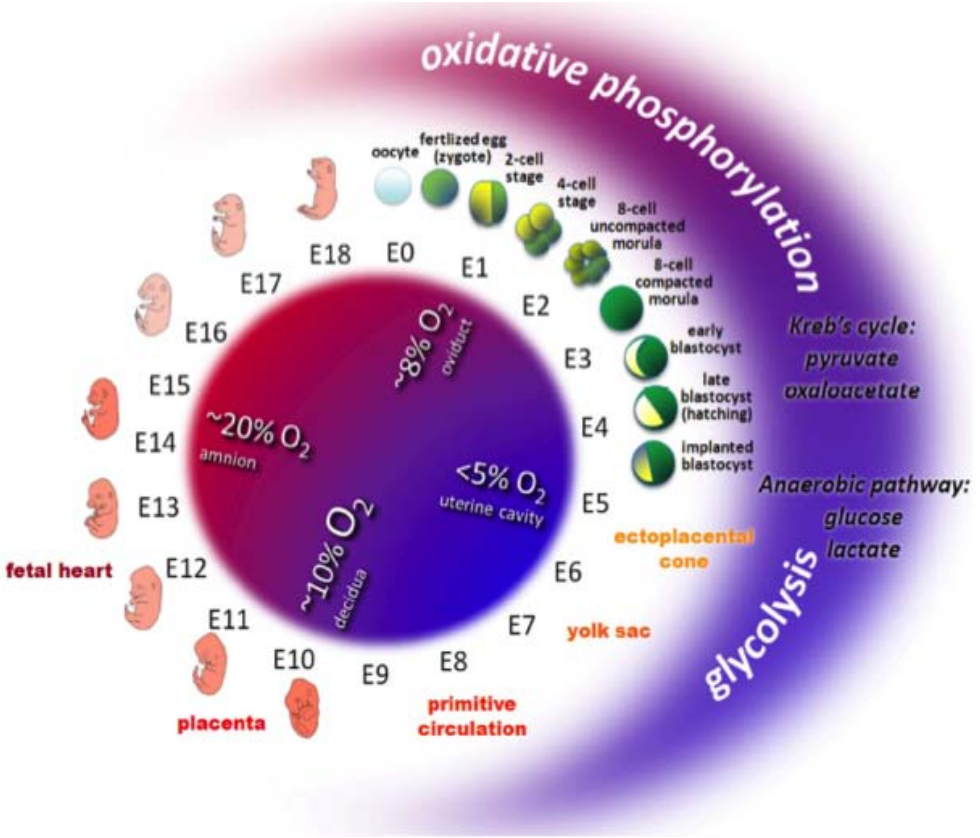

Ufer and Wang. Front. Mol. *Neurosci*., 28 July 2011

Conflict of interest disclosure: cofounder of Embryologic

Activity of Metabolic Cofactor NADH during Pre-implantation Embryo Development

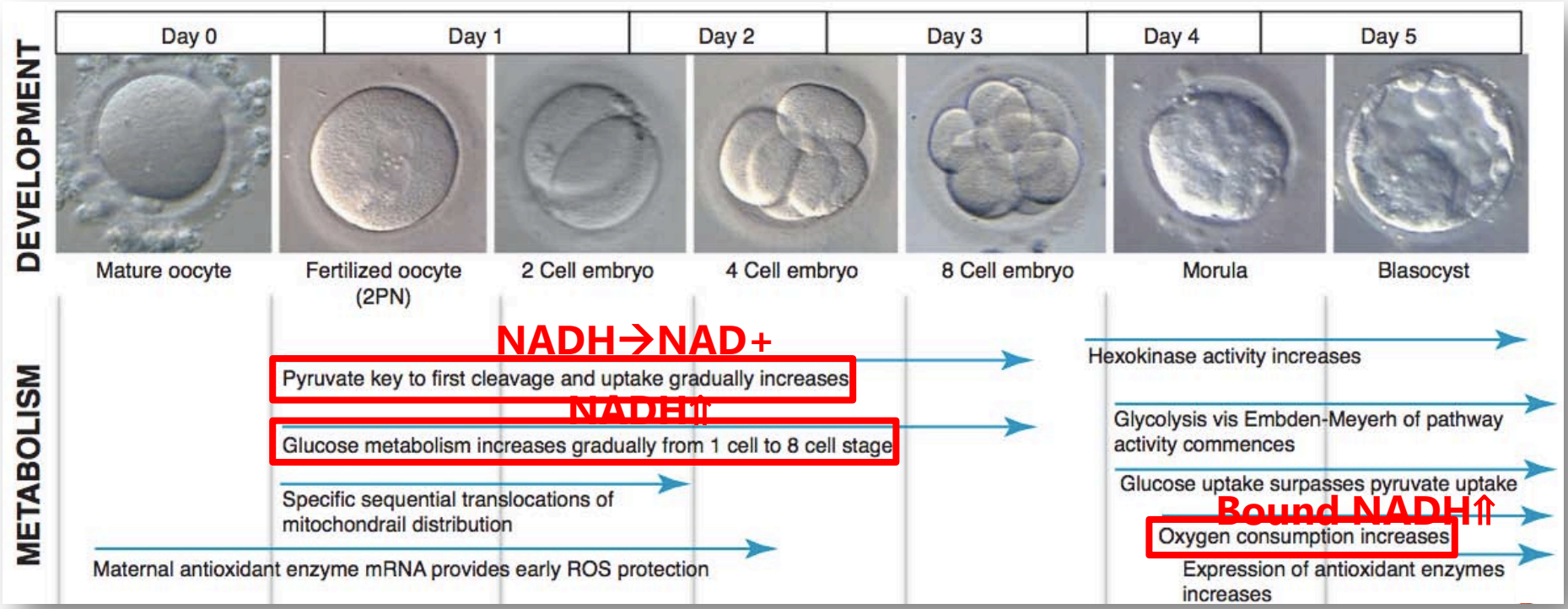

- **Nicotinamide adenine dinucleotide(NADH)**
- **Endogenous fluorescent**
- **Plays a key role in production of energy in cells and tissues**
- **Oxidized form (NAD+) of the coenzyme does not fluoresce**

Chason et al., 2011

Metabolism was found to be associated with viability

- **Studies of the embryonic developmental in multiple mammalian species shows glucose uptake correlates to embryo health**

Mouse Blastocyst

TABLE 1. The uptake of glucose (1 mM) by single mouse blastocysts prior to transfer into pseudopregnant recipients[a]

Glucose uptake (pmol/embryo/hour)		
Male	Female	Nonviable
4.37 ± 0.22[b]	4.92 ±0.36	3.57 ± 0.46

Gardner and Leese, 1987

Human Blastocyst

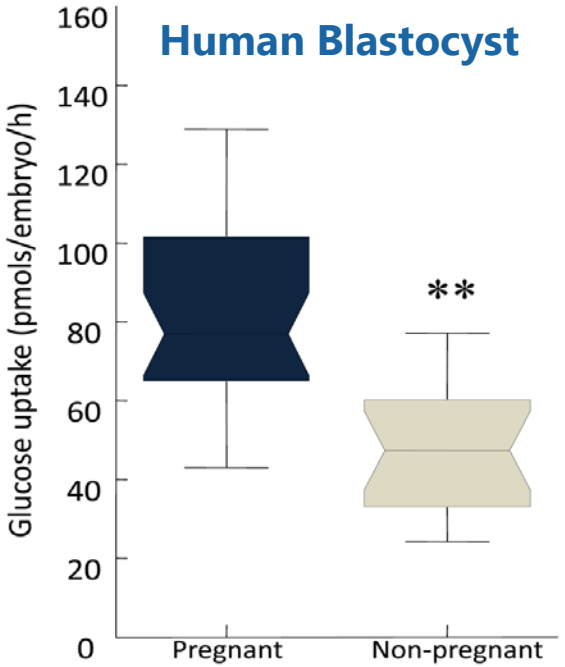

Gardner, 2015

Bovine Blastocyst

Development of cultured bovine embryos after single cervical transfer

	Embryos showing glucose uptake	Embryos with no glucose uptake	Total
No. of recipients	13	14	27
No. of pregnancies at Day 50	9*	2*	11
(%)	(69.2)+	(14.2)	(40.7)

* Significantly different (x^2=6.30; P < 0.025).
\+ Including 1 dead fetus

Renard et al. , 1980

Imaging Strategy:

Non-invasive Phasor-FLIM mouse preimplantation embryo model

1. Superovulation and Embryo Collection

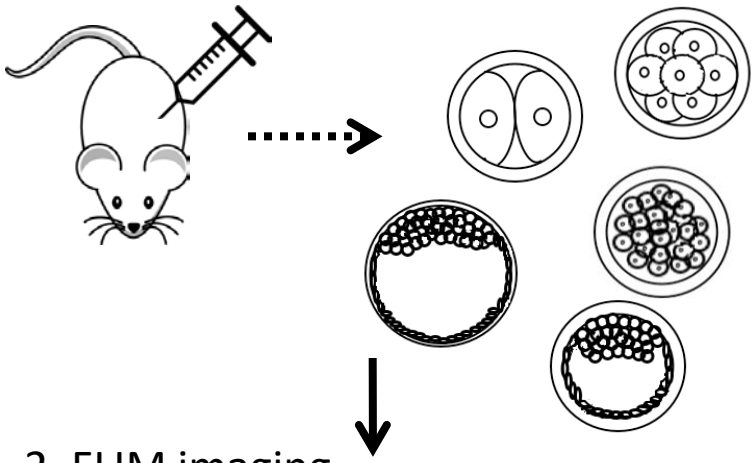

2. FLIM imaging

- Non-inbred CD-1 and Inbred C57BL/6
- 24-day old females
- Superovulation with PMSG and hCG

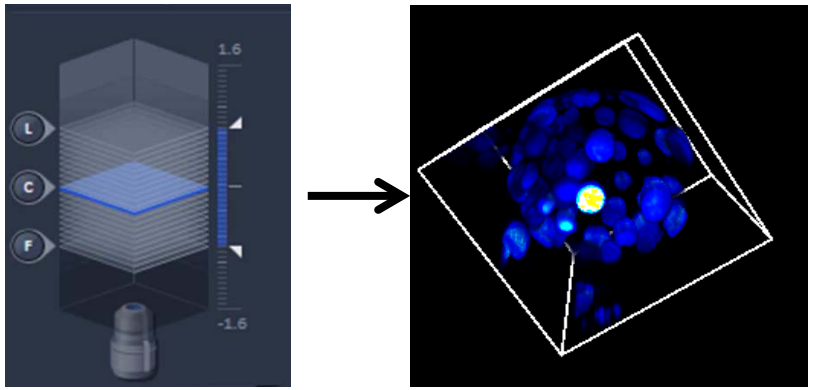

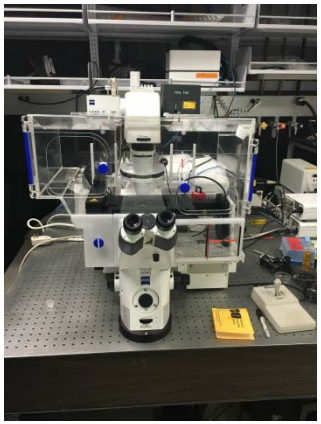

- Zeiss LSM710 + Fast FLIM data acquisition card
- Zeiss EC Plan-Neofluar 20x/0.5 NA objective
- Excitation/Emission: 740nm/420-500nm
- ~3.5mW laser power
- 50 frames z-stack integration (~3 minute)
- 37 °C, 5% CO_2

Progression of ROS production shifts the lifetime towards the oxidized lipid lifetime

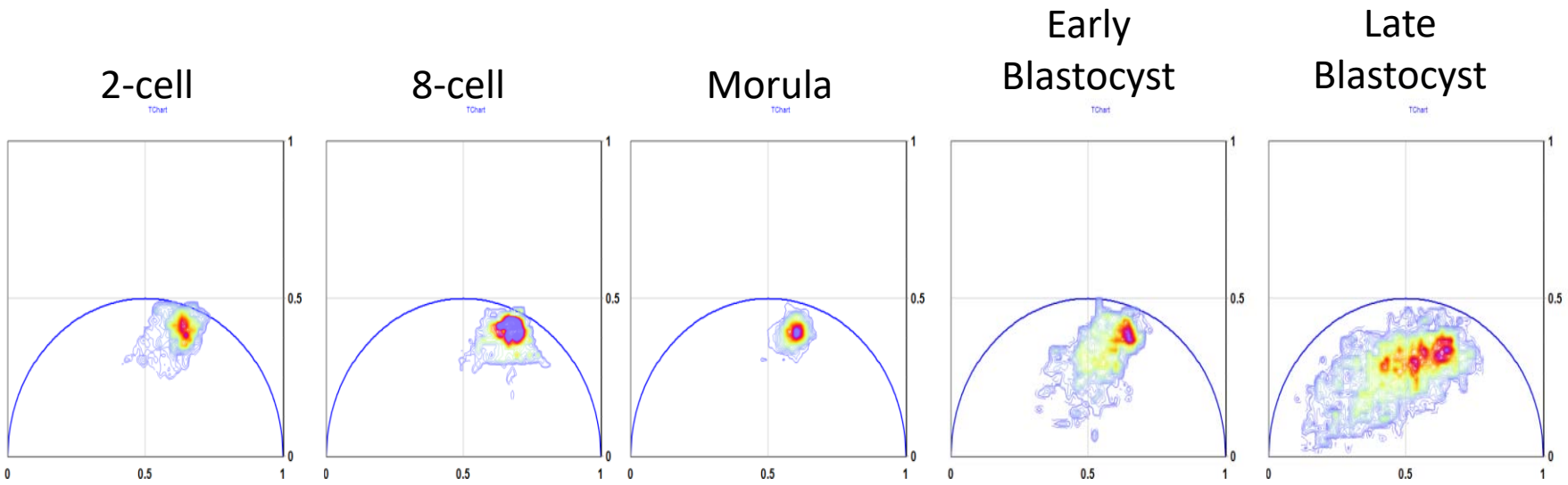

- In bovine embryos by 8-cell stage, ROS levels increase, and then they decrease by the blastocyst stage (Dalvit, 2005).
- Production of ROS, or increase of free radicals, is a normal result of cellular metabolism responsible for maintaining a good redox balance

Lifetime population trajectory of healthy developing embryos

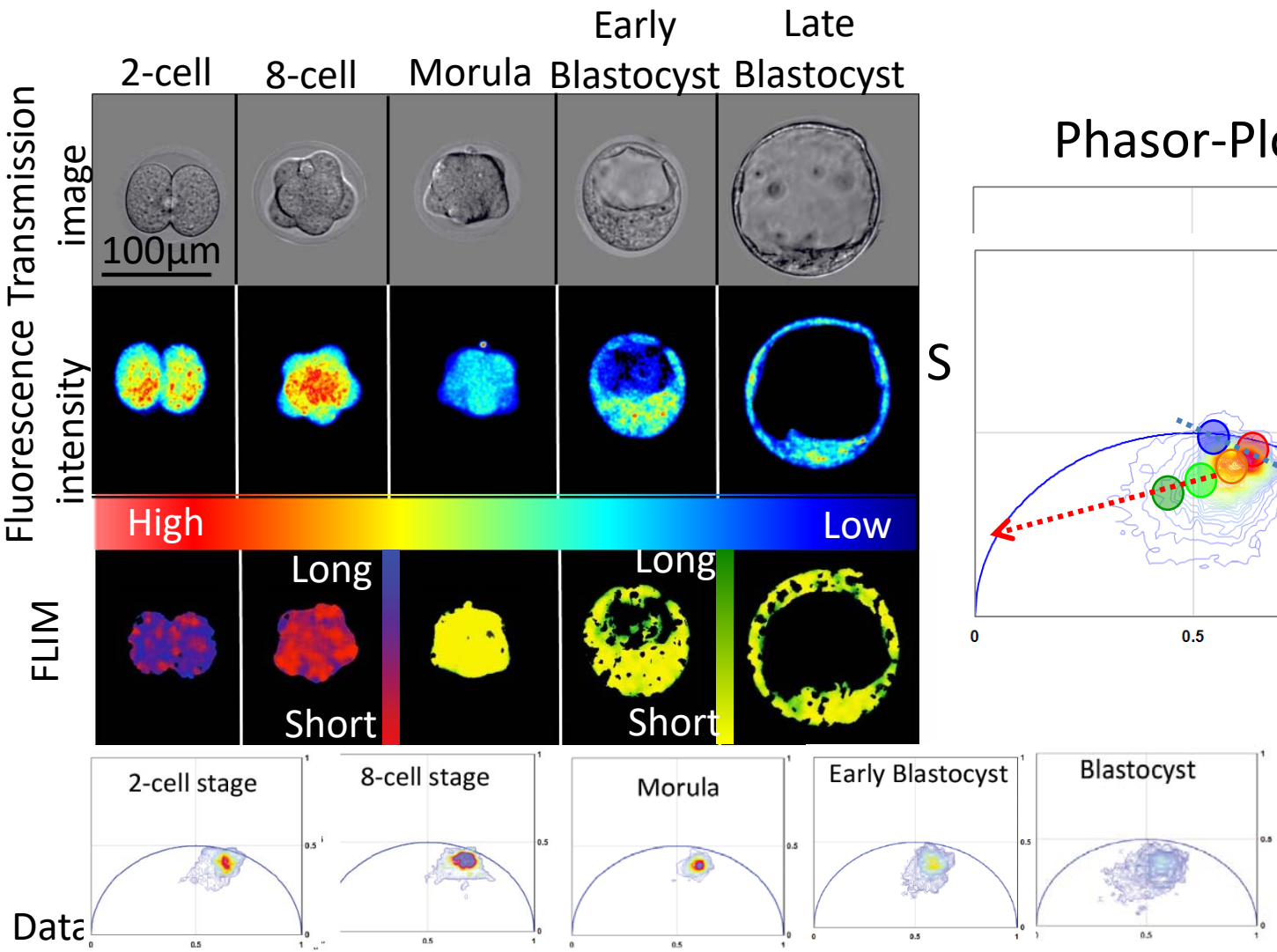

Ma N , et al, Scientific Reports, 2019; 9(1), 13206.

Lifetime population trajectory of healthy developing embryos

Stage	Major metabolism in literature	Expected NADH signature
2-cell	Pyruvate uptake (Biggers et al. ,1967, Whitten et al., 1957, Brinster et al., 1965)	free NADH↓
Late 4-cell/8-cell	Glycolysis (Brinster et al. ,1966)	free NADH⇧
Blastocyst	Oxidative phosphorylation (Gardner et al, 2010, Lane et al. 1996, Gardner et al. 1987)	Bound NADH⇧

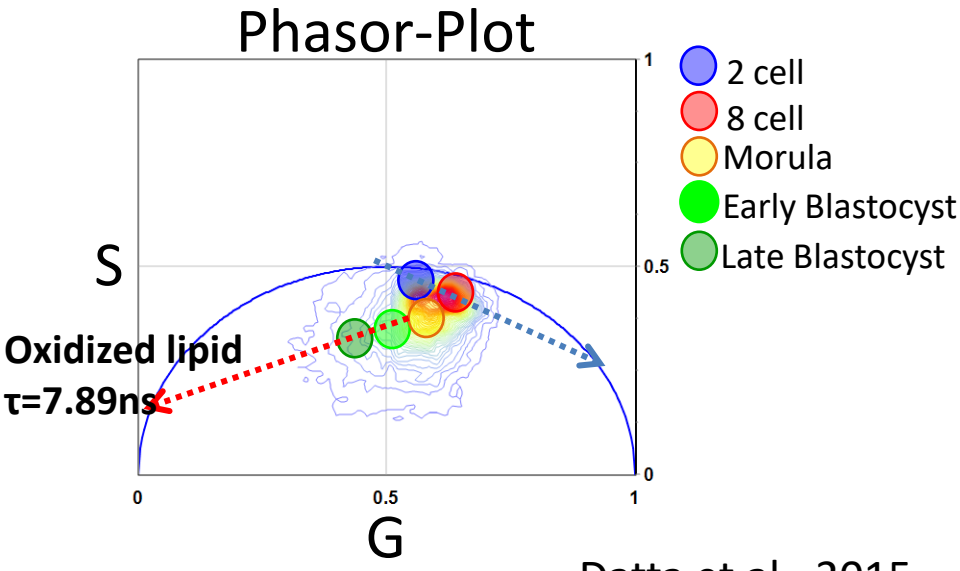

Datta et al., 2015

Lifetime:

Long → Short → Long

Phasor-FLIM can measure metabolism during embryonic development in pre-implantation embryos

Long lifetime species (LLS): FLIM signature and a new oxidative stress axis on phasor

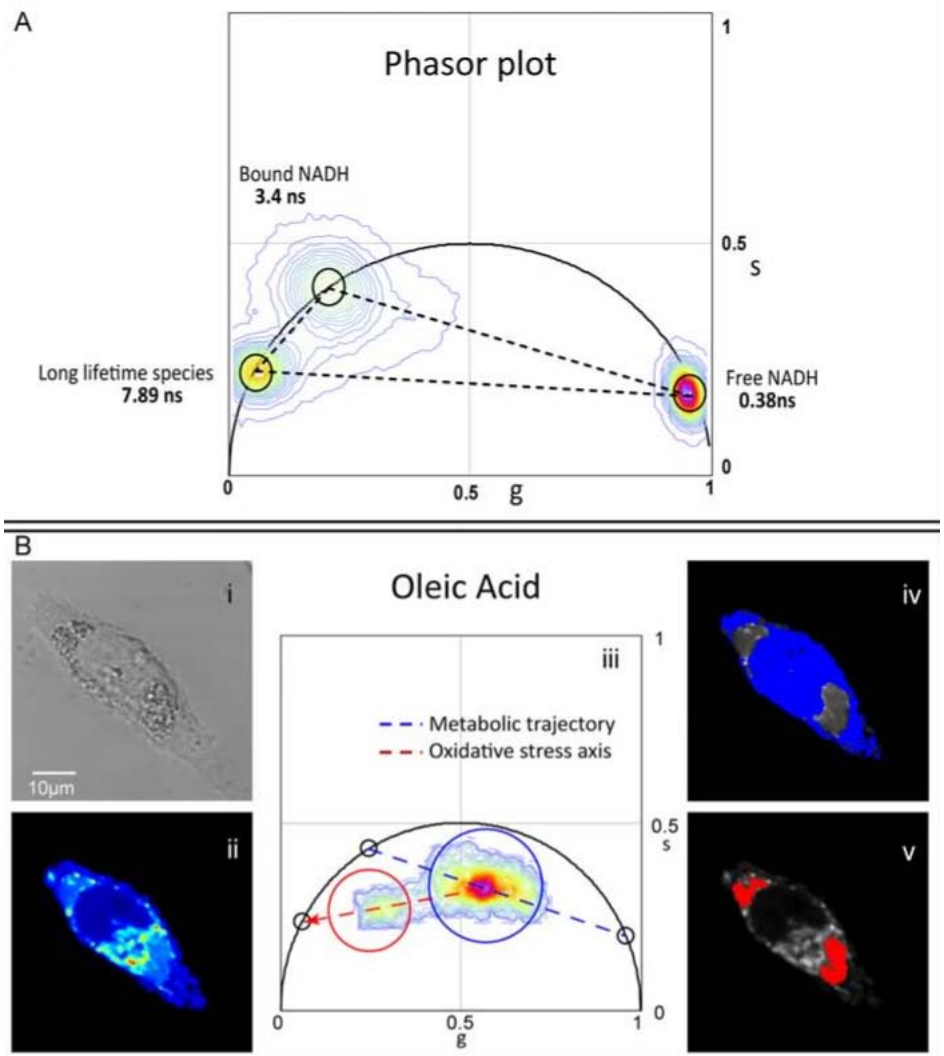

Datta R., Alfonso-García A., Cinco R., Gratton E. (2015) Sci. Rep. 5:9848.

Why is ROS production needed for embryonic development?

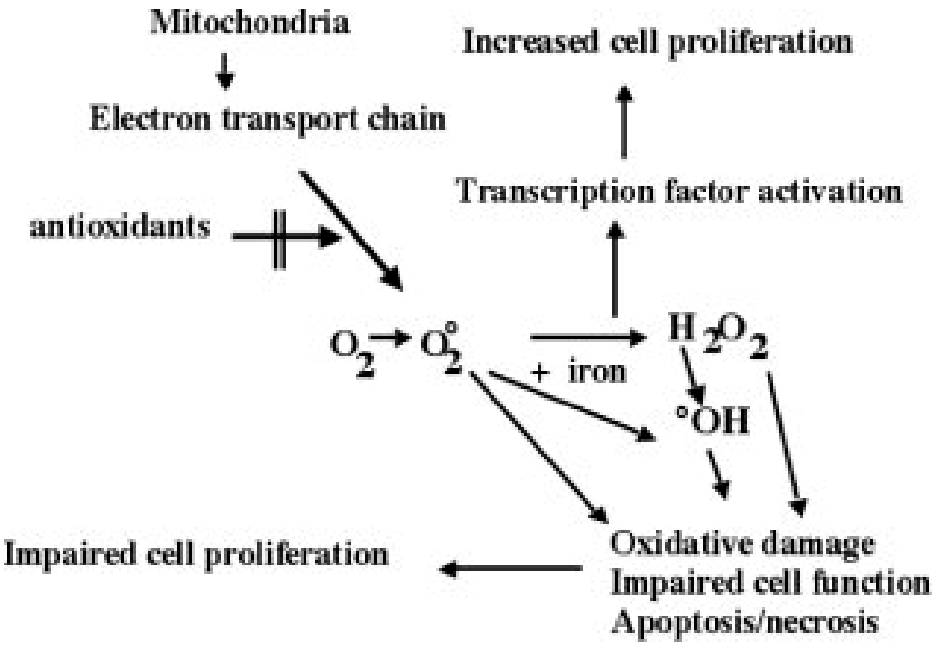

- In bovine embryos by 8-cell stage, ROS levels increase, and then they decrease by the blastocyst stage . Production of ROS, or increase of free radicals, is a normal result of cellular metabolism responsible for maintaining a good redox balance

- ROS are important in normal development through cellular signaling and control of cellular fate.

Reactive Oxygen Species (ROS) detection

- DCF-DA: Reactive Oxygen Species
- 3rd

Blue: DAPI
Green: DCF-DA

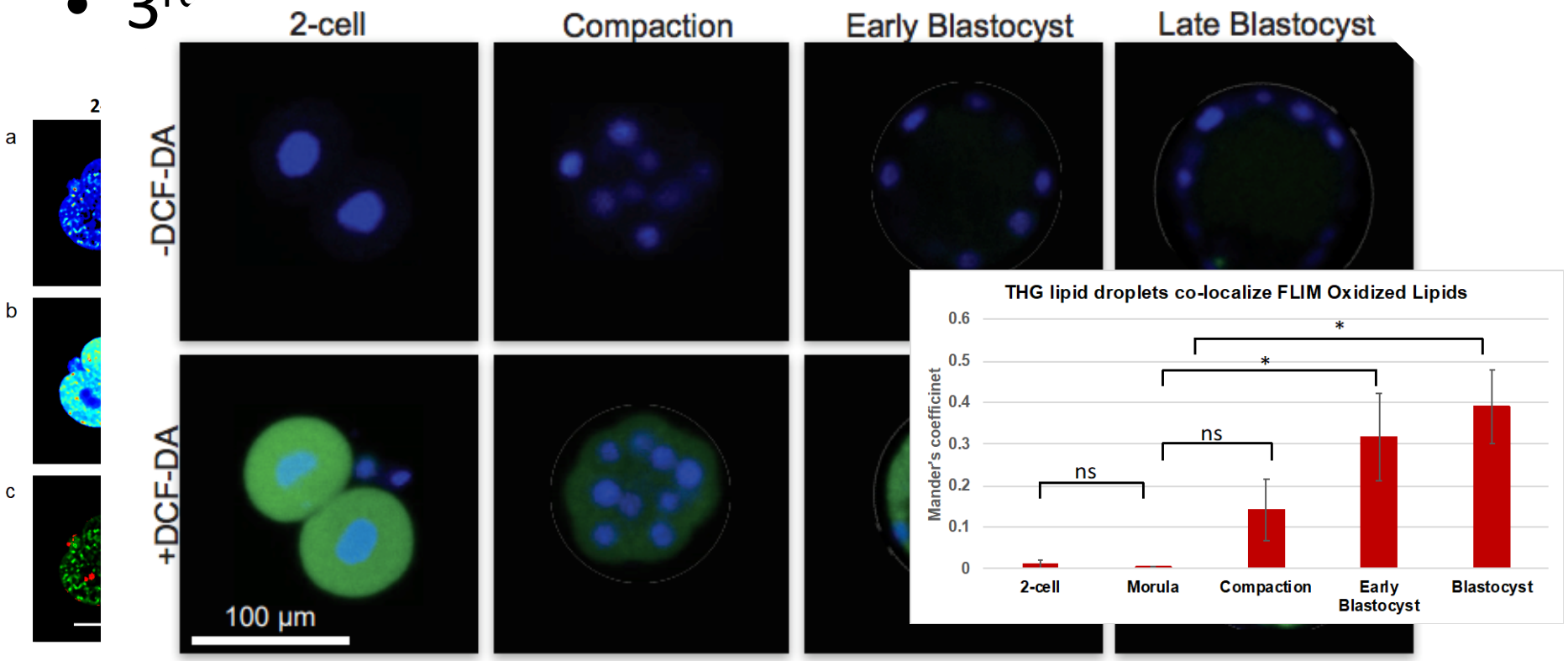

Manipulation of embryo metabolism

- Rotenone and Antimycin A (R&A): Oxidative Phosphorylation inhibitor

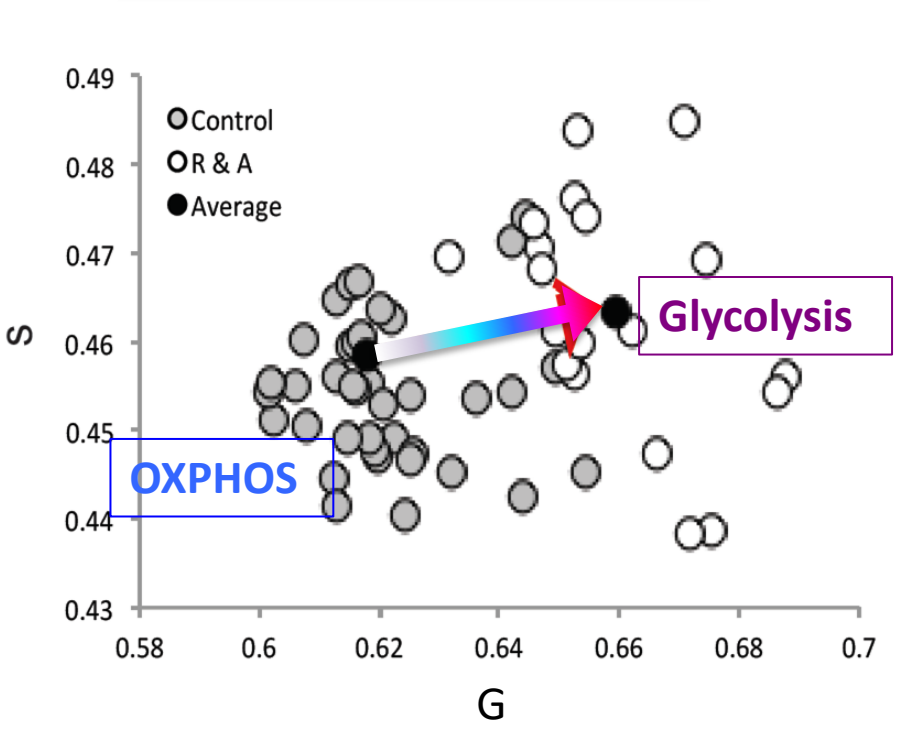

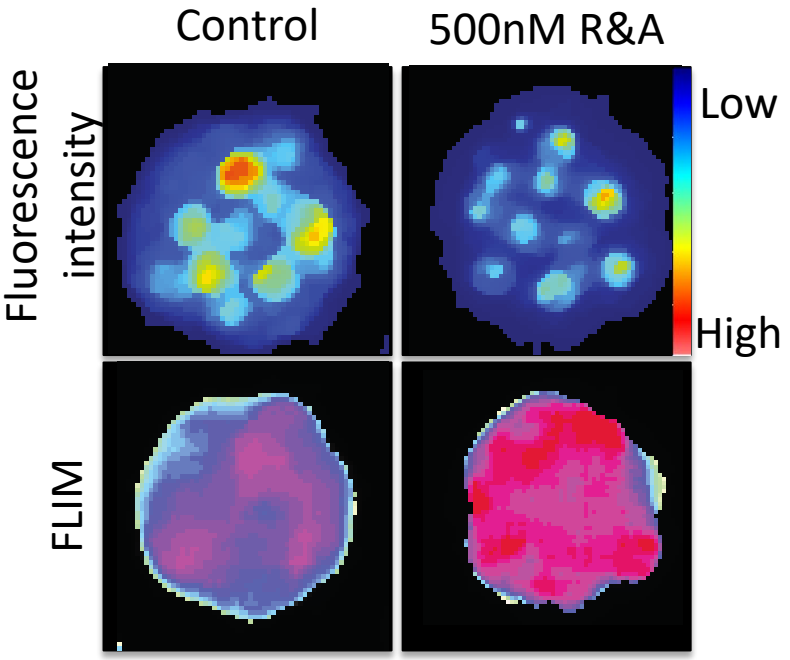

Ma N , et al, Scientific Reports, 2019; 9(1), 13206.

Manipulation of embryo metabolism

- 2 Deoxy-D-Glucose (2DG): Glycolysis inhibitor

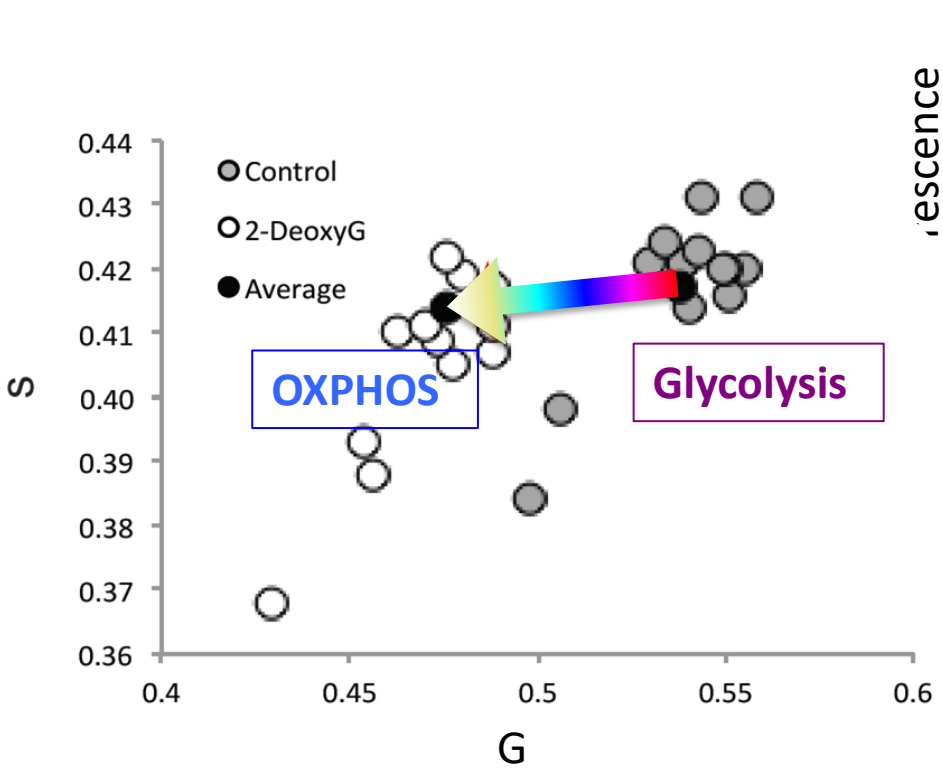

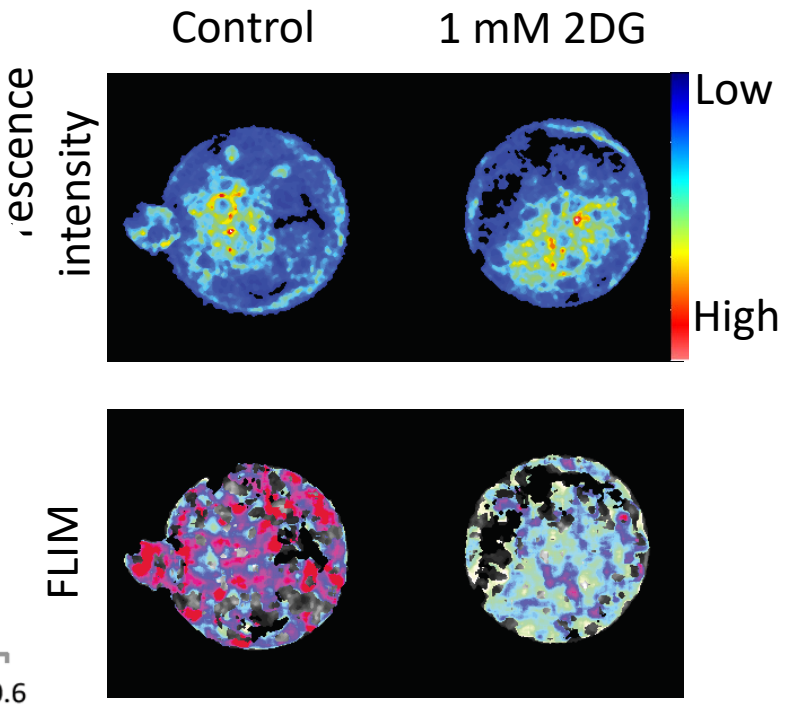

Ma N , et al, Scientific Reports, 2019; 9(1), 13206.

FLIM can distinguish healthy embryos and the embryos under “high stress” conditions

After 24 hour treatment

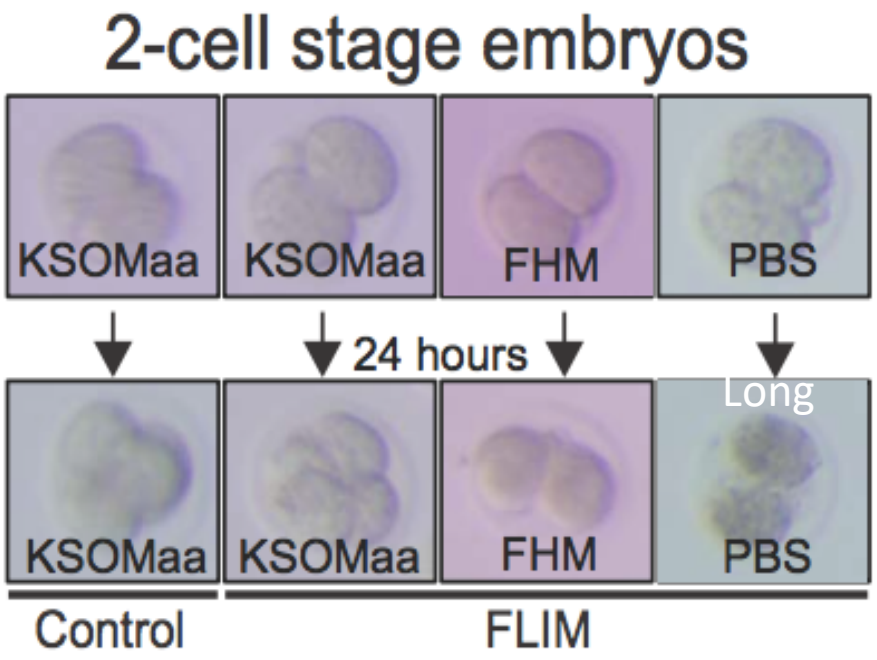

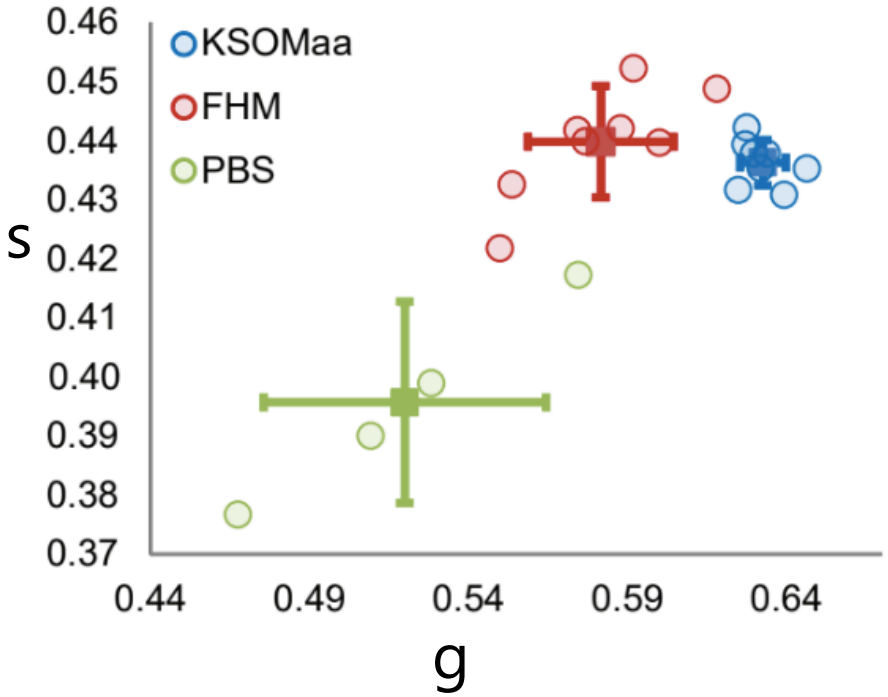

KSOMaa: standard culture media

FHM: nutrient lacking flushing and holding media

PBS: saline solution

Ma N , et al, Scientific Reports, 2019; 9(1), 13206.

Can we use the phasor/FLIM method to predict the best developmental potential for each embryo?

1. Superovulation

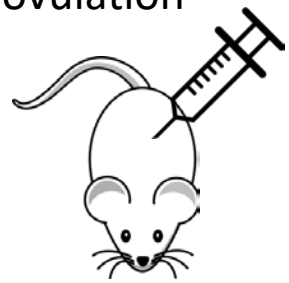

2. Embryo Collection (2-cell stage)
40~180 embryos for each experiment

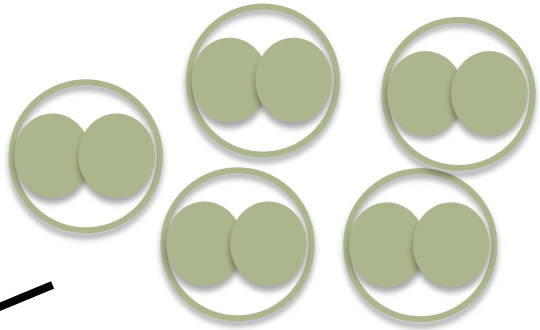

3. FLIM imaging and Time-lapse
Imaging for ~60 hours

Ma N, et al; Sci Rep. 2019; 9(1), 13206. PMCID: PMC6744410

Time-lapse imaging of a healthy (H) and an “unhealthy” (UH) preimplantation embryo

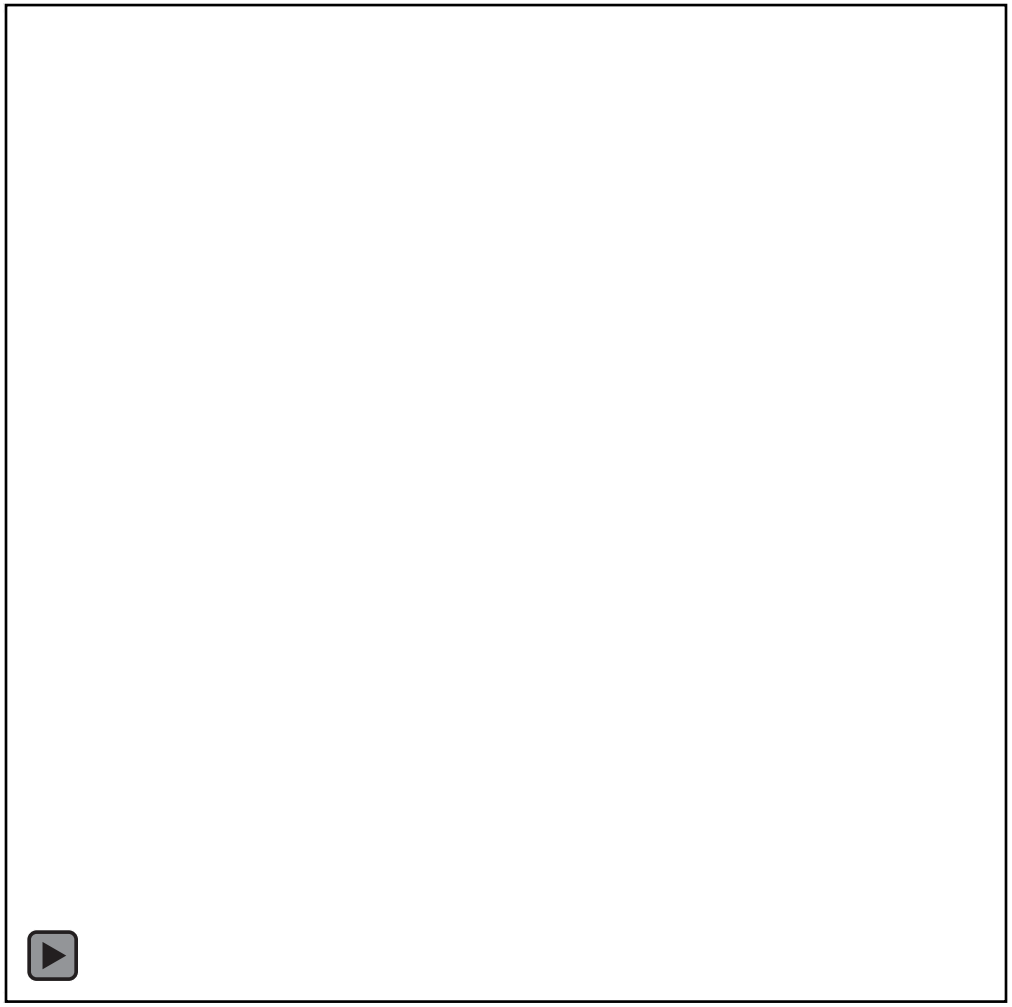

H: Embryos developed to blastocyst

UH: Embryos arrested before blastocyst at morula stage

The “Distance” analysis approach of the phasor plot

Premise: the phasor plot contains about 10,000 points for each image and generally we analyze 10 to 100 images all together

At 8 cell stage the embryos appear to be indistinguishable through 2D phasor

Control Survived

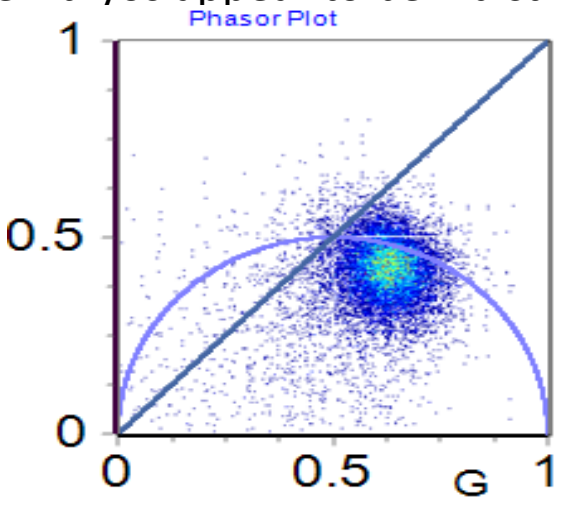

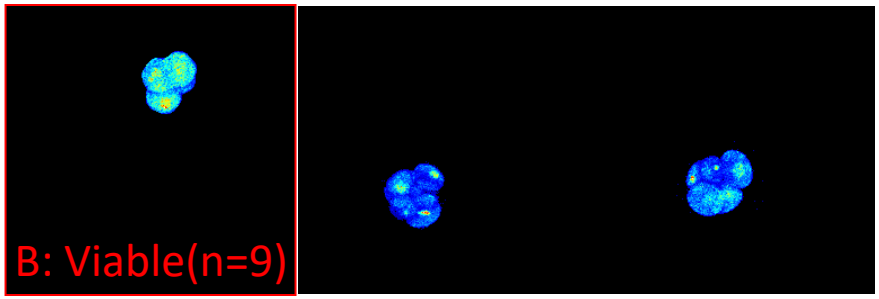

Known
Did not survive

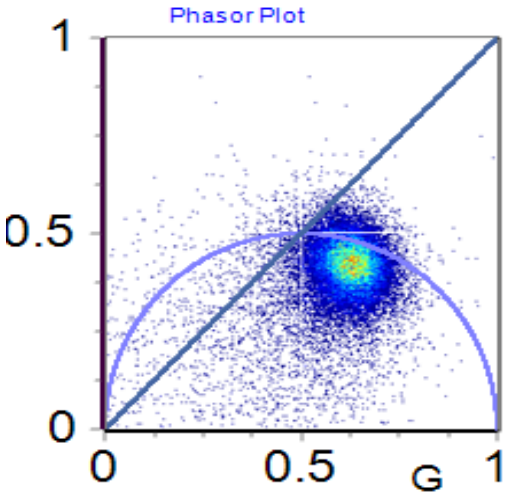

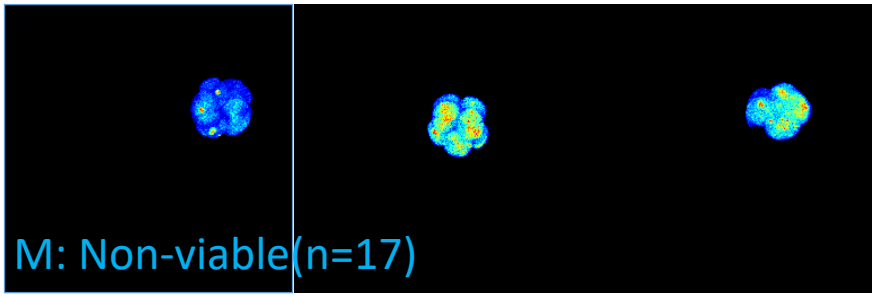

Combination of FLIM imaging and time-lapse morphological tracking work flow

1. Superovulation

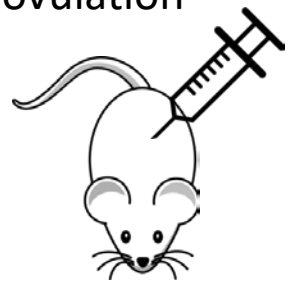

2. Embryo Collection (E1.5)

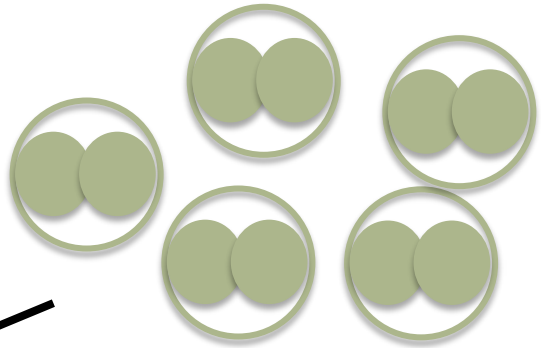

3. FLIM imaging and Time-lapse Imaging for ~60 hours

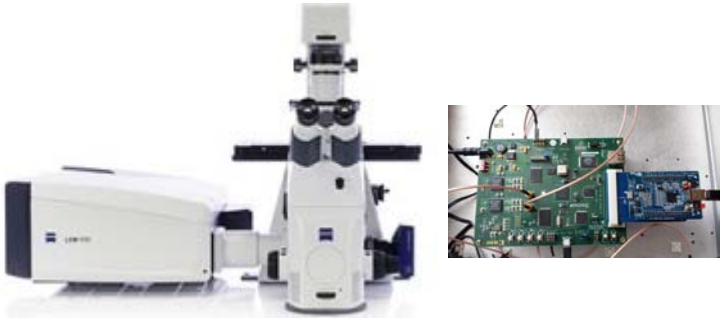

4.Distance-

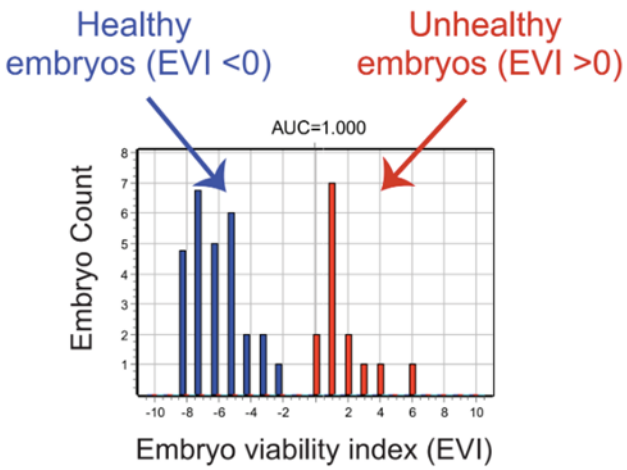

Ma N, et al; Sci Rep. 2019; 9(1), 13206. PMCID: PMC6744410

FLIM does not cause DNA damage

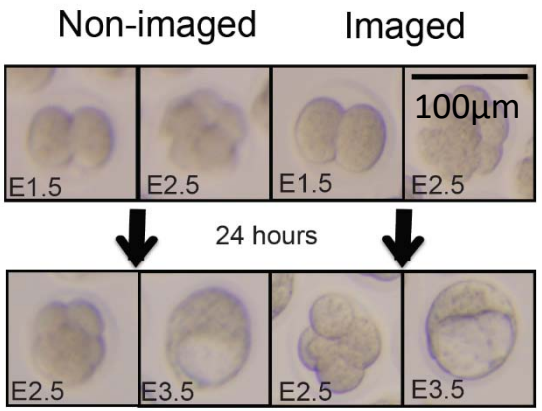

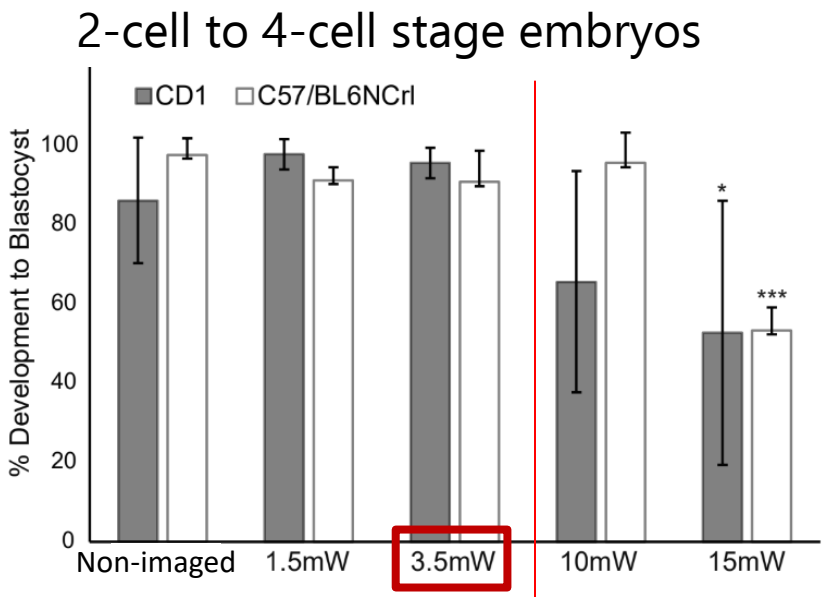

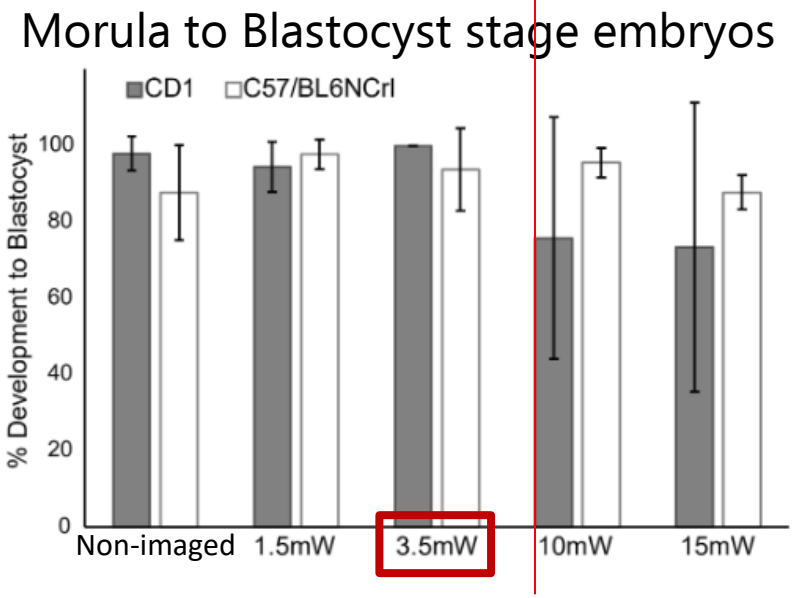

3.5mW: average laser power for embryo imaging (50 frames)

Ma N, et al; Sci Rep. 2019; 9(1), 13206. PMCID: PMC6744410

Principle of absolute NADH concentration measurement

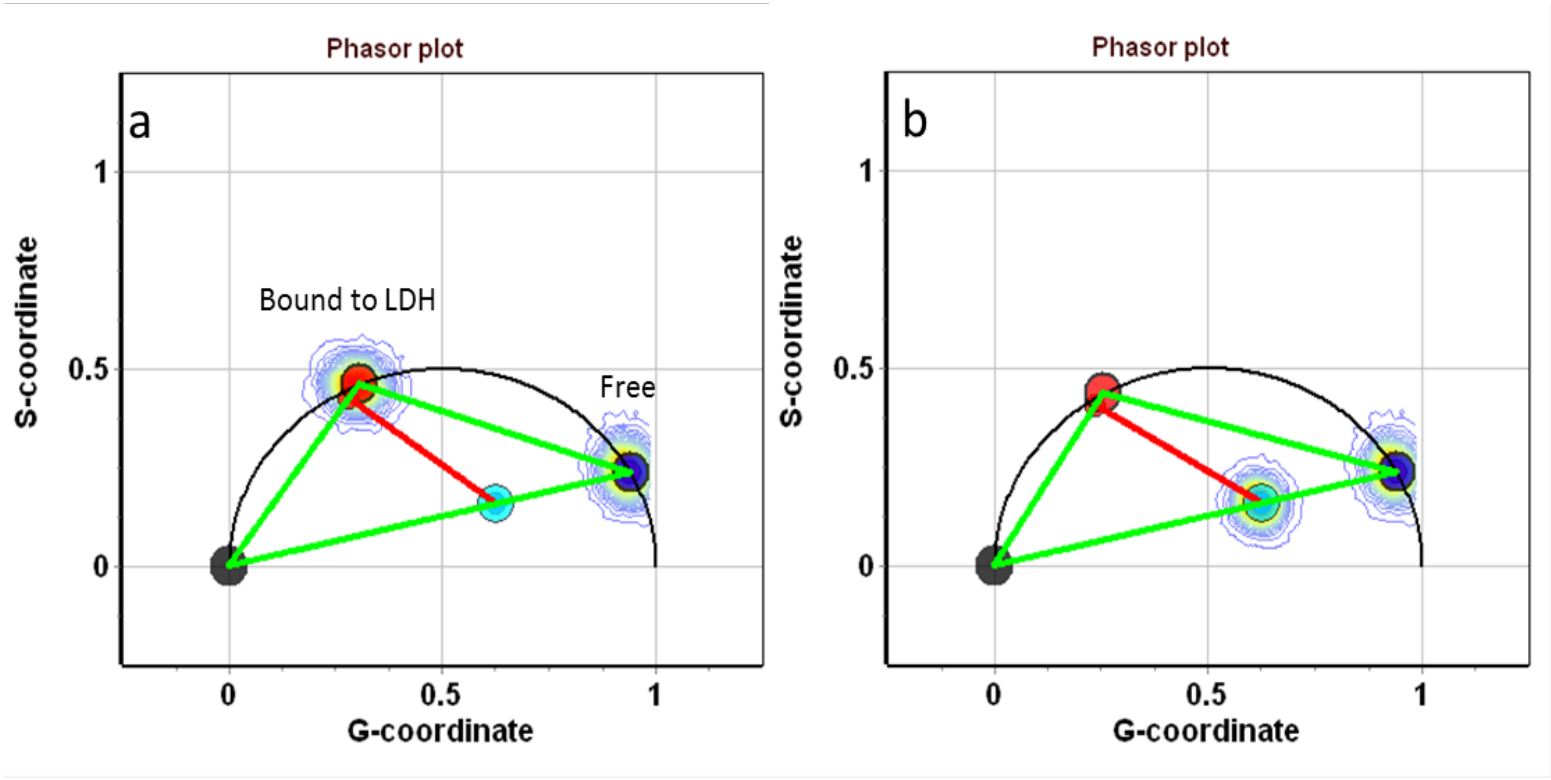

$$M = \frac{L}{L+F}$$

g: experimental g

g_0: g coordinate of the calibration solution without external light added

M: modulation of phasor

L: intensity of unmodulated light

F: intensity of fluorescence of the specimen

g: experimental g

g_0: g coordinate of the calibration solution without external light added

M: modulation of phasor

L: intensity of unmodulated light

F: intensity of fluorescence of the specimen

Ma et al. Biomed Opt Express. 2016; 7(7): 2441-2452.

Absolute NADH concentration measurement in Cho-K1 cells

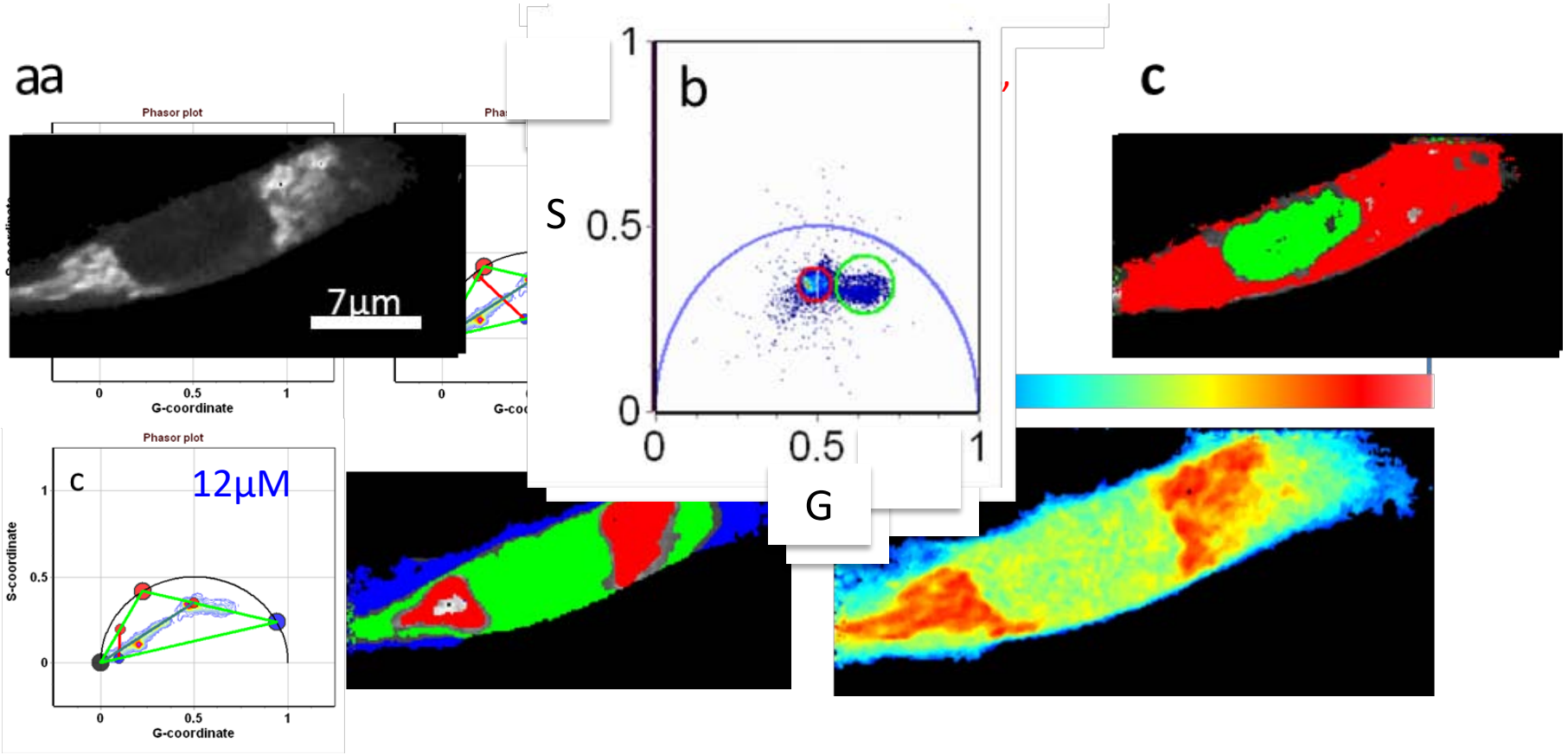

The method only requires the measurement of a solution of NADH at a known concentration

Previous measurement of NADH concentration in normal cells and cancer cells are in the range **97μM-168μM**, the values demonstrate our method can derive absolute NADH concentration in cells (Klaidman et al. 1995, Yu et al., 2009)

Ma et al. Biomed Opt Express. 2016; 7(7): 2441-2452.

Preliminary data for NADH absolute concentration during embryonic development

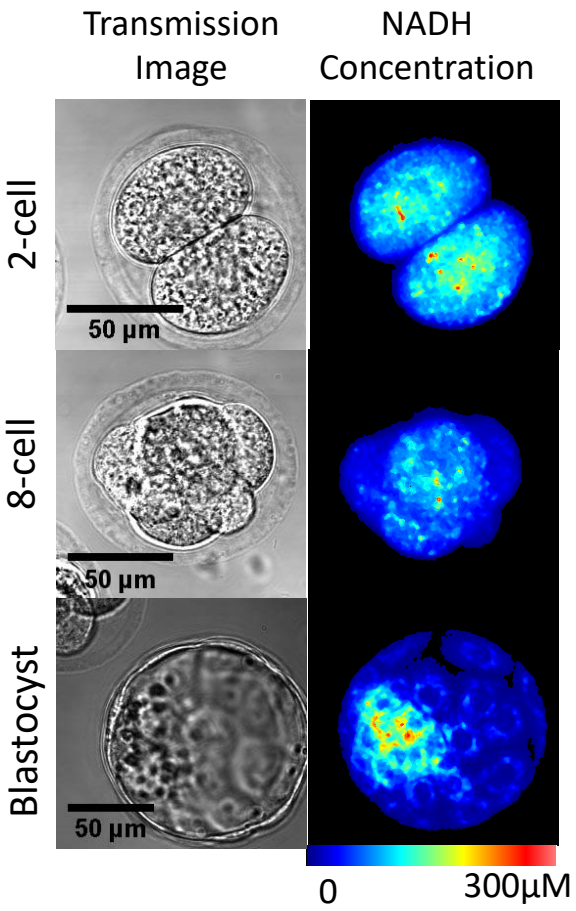

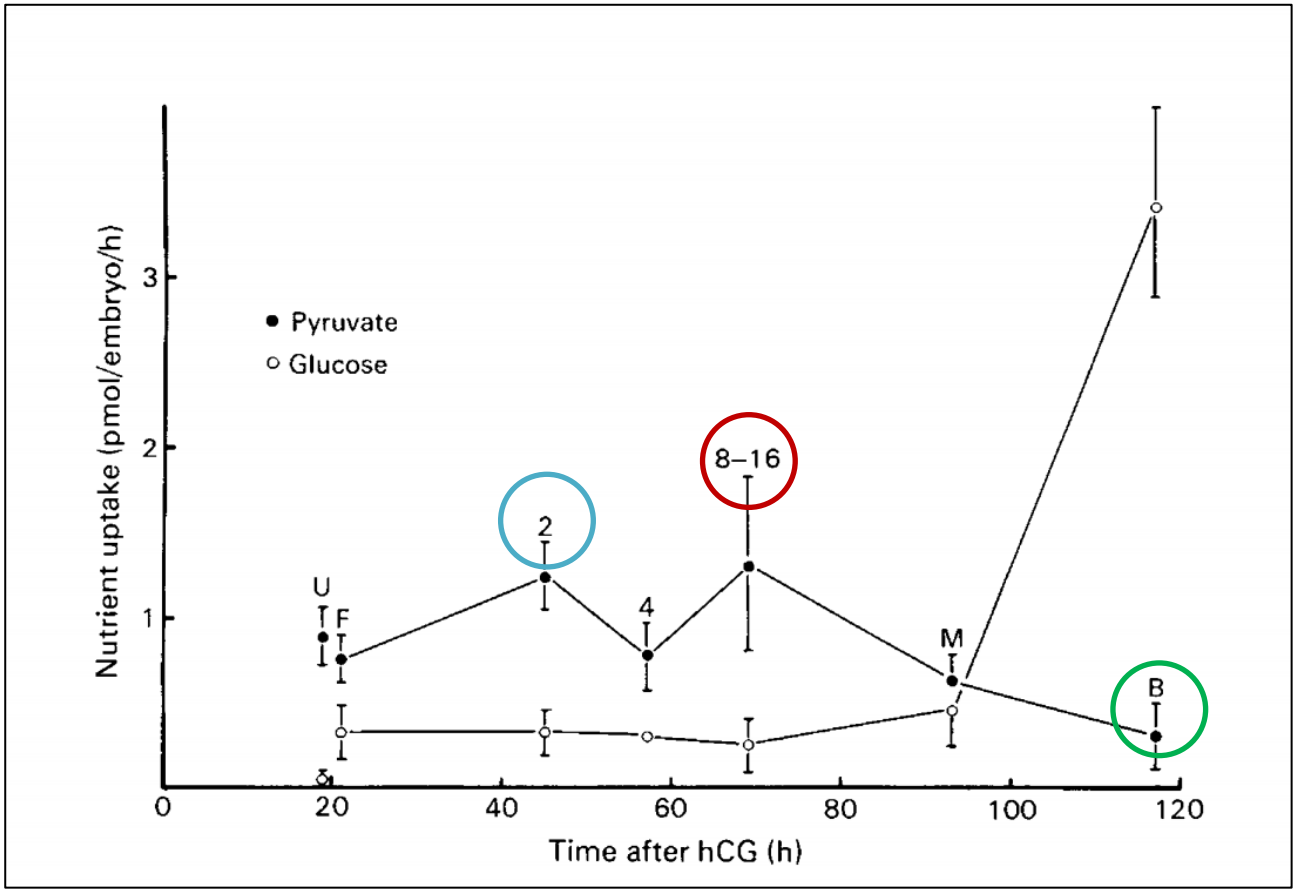

Data collected by Ning Ma

Leese et al., 1984

Comparing absolute NADH concentration in healthy embryos and embryos under “high stress”

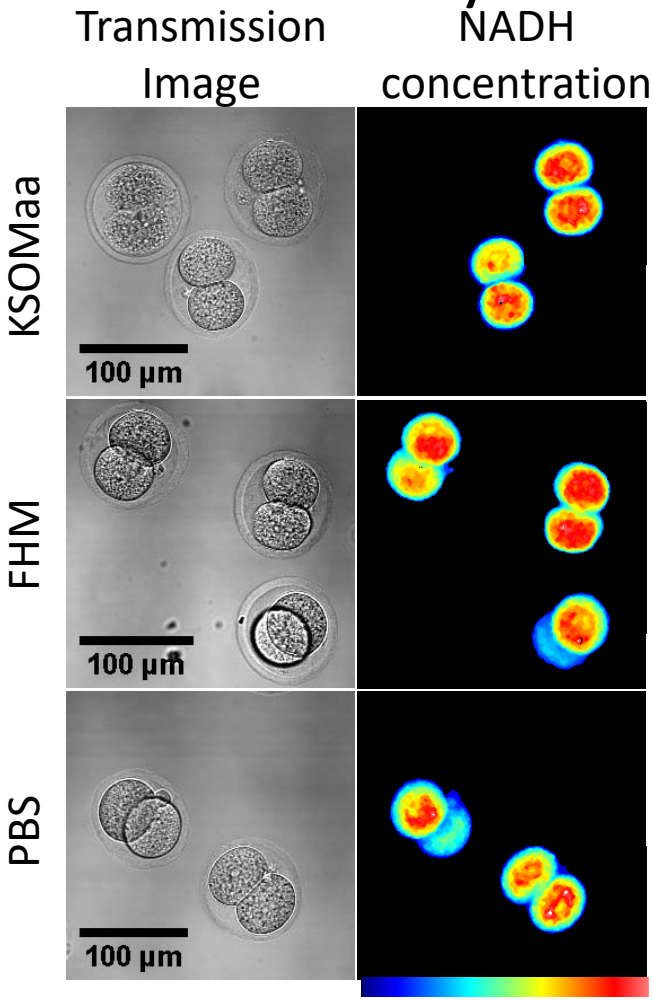

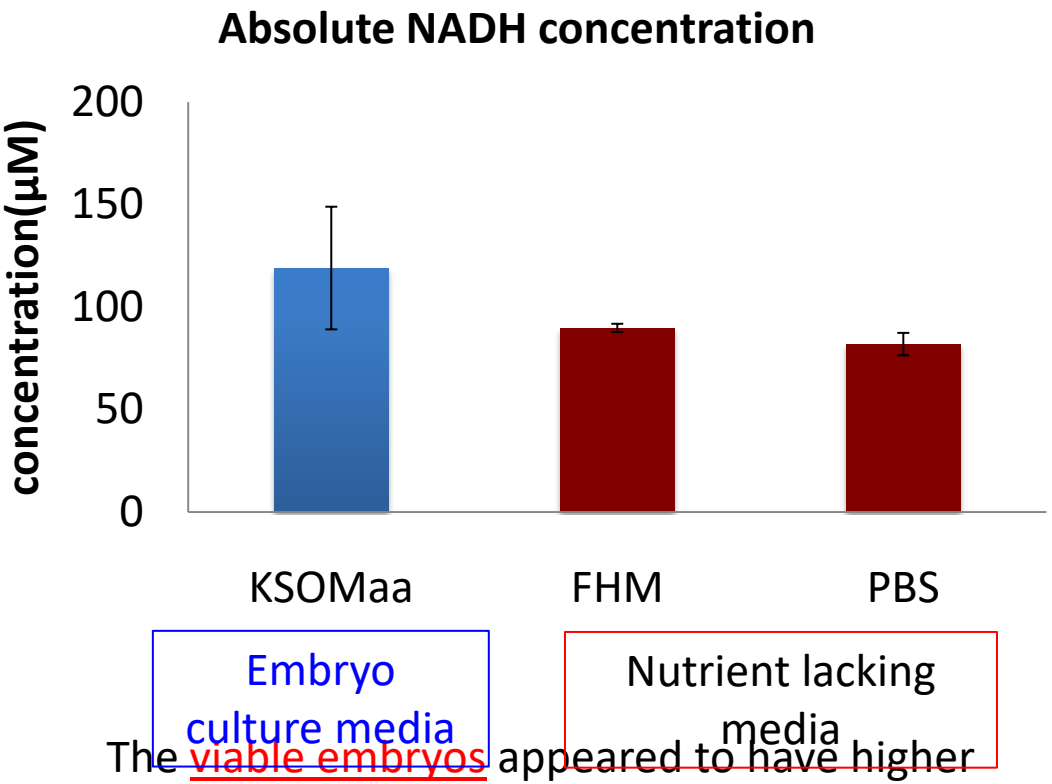

The viable embryos appeared to have higher NADH level.

Data collected by Ning Ma

Embryo viability prediction Pipeline

MENU SCIENTIFIC REPORTS

Article | Open Access | Published: 13 September 2019

Label-free assessment of pre-implantation embryo quality by the Fluorescence Lifetime Imaging Microscopy (FLIM)-phasor approach

Ning Ma, Nabora Reyes de Mochel, Paula Duyen Pham, Tae Yeon Yoo, Ken W. Y. Cho & Michelle A. Digman

Scientific Reports **9**, Article number: 13206 (2019) | Cite this article

677 Accesses | **4** Altmetric | Metrics

Summary

- Mouse pre-implantation embryo has unique lifetime trajectory during development which can be detected by Phasor-FLIM noninvasively and quantitatively

- 8-cell stage is the optimal stage for the prediction

- FLIM can be a useful tool to detect embryo viability

The Digman Lab

Metabolic Alterations

Embryo Development
Neurodegeneration
Cancer

Mechanobiology and the Influence of ECM on Metabolism in Cancer Cells

Mitochondrial recruitment
Tumor organoids

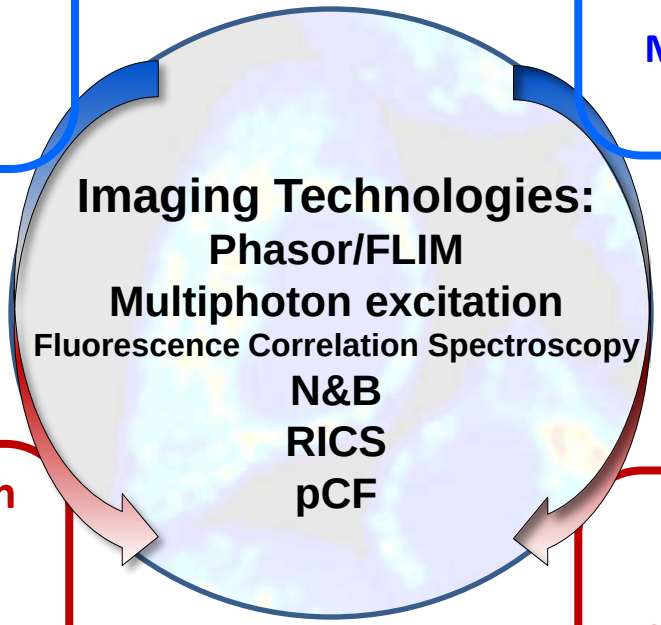

DNA Damage and Protein Phase Transitions in Health and Disease

Protein dynamics and distinct physical states

Signal transduction dynamics during epidermal wound healing and partial Epithelial-to-Mesenchymal Transition

Acknowledgements

Austin Lefebvre

Angel Balam Benitez Mata

Yu-Kai Huang

COLLABORATORS:

Greg Brewer

Yue Dong

DGE-1839285
(Austin Lefebvre)

Career Award #1847005
(Dr. Digman)

Ken Cho

Soledad Mochel

Paula Pham

Tommy Yoon